Chapter 4

Article 2

Arzneimittelforschung/Drug Research

Structure-activity relationships for the inhibition of monoamine oxidase by 8-(2-phenoxyethoxy)caffeine analogues

Belinda Strydom[a], Jacobus J. Bergh[a], Jacobus P. Petzer[a]

[a]Pharmaceutical Chemistry, School of Pharmacy, North-West University, Private Bag X6001, Potchefstroom 2520, South Africa

Arzneimittelforschung, Accepted manuscript.

Graphical abstract:

The synthesis of 8-(2-phenoxyethoxy)caffeine analogues with increased potency towards both MAO-A and –B compared to the lead compound, **3a**.

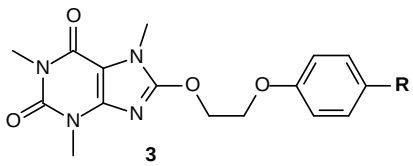

3

		IC_{50} values (μM)	
Compd.	**R**	MAO-A	MAO-B
3a	-H	20.4 ± 16.5[a]	0.383 ± 0.021[a]
3e	$-CF_3$	2.22 ± 0.068	0.061 ± 0.003
3h	-I	0.924 ± 0.031	0.128 ± 0.013

[a] Values obtained from literature (Strydom et al., 2011).

Structure-activity relationships for the inhibition of monoamine oxidase by 8-(2-phenoxyethoxy)caffeine analogues

Belinda Strydom [a], Jacobus J. Bergh [a], Jacobus P. Petzer [a]

Abstract—Previous studies have documented that substituted 8-oxycaffeines are potent reversible and selective inhibitors of human monoamine oxidase (MAO) B. A particularly potent inhibitor among the reported compounds was 8-(2-phenoxyethoxy)caffeine with an IC_{50} value of 0.383 µM towards MAO-B. It was also reported that halogen substitution at C4 of the phenoxy ring leads to an enhancement of both MAO-A and –B inhibition potencies. In an attempt to discover highly potent reversible MAO-B inhibitors and to examine the structure-activity relationships (SAR) of MAO inhibition by these compounds, in the present study a series of 8-(2-phenoxyethoxy)caffeine analogues containing various substituents at C4 of the phenoxy ring were synthesized and evaluated as inhibitors of human MAO-A and –B. The results show that the 8-(2-phenoxyethoxy)caffeine analogues are selective MAO-B inhibitors with the most potent homologue, 8-{2-[4-(trifluoromethyl)phenoxy]ethoxy}caffeine, exhibiting an IC_{50} value of 0.061 µM. A quantitative structure-activity relationship (QSAR) study indicates that substitution with electron withdrawing and lipophilic functional groups on C4 of the phenoxy ring enhances the inhibition potencies towards both MAO-A and –B. Interestingly, an increase in size of the substituent at C4 correlates with an enhancement in MAO-A inhibition potency while less bulky groups are favourable for MAO-B inhibition. The binding orientations of selected compounds within the active site cavities of MAO-A and –B are also examined.

[a] *Pharmaceutical Chemistry, School of Pharmacy, North-West University, Private Bag X6001, Potchefstroom, 2520, South Africa.*

4.1. Introduction

Monoamine oxidase (MAO) is a flavin adenine dinucleotide (FAD) containing enzyme which is bound to the outer mitochondrial membrane. MAO is classified into two distinct isoforms, MAO-A and –B, which share a 70% sequence identity and are products of separate genes [1,2]. The principal function of the MAO isozymes is the oxidative deamination of primary amines of an endogenous and dietary nature. In the central en peripheral tissues, MAO is responsible for the termination of the action of neurotransmitter amines such as serotonin, dopamine, epinephrine and norepinephrine [1,3]. The two MAO isoforms may be distinguished by their different substrate specificities. MAO-A preferentially catalyzes the oxidation of serotonin while MAO-B favors benzylamine and 2-phenethylamine as substrates [3]. Dopamine, epinephrine, norepinephrine and tyramine are considered to be substrates for both MAO isoforms [3].

MAO has acted as a target for the treatment of central nervous system diseases [3,4,5]. Selective MAO-A inhibitors are reported to be effective in the treatment of depression by increasing the levels of serotonin, norepinephrine and dopamine in the brain [4]. An example of such a drug is the reversible MAO-A inhibitor, moclobemide [6]. Since MAO-B is considered to be the major dopamine metabolizing enzyme in the basal ganglia of the brain, MAO-B inhibitors are used in the treatment of Parkinson's disease [7,8]. In the basal ganglia, inhibitors of MAO-B are thought to reduce the depletion of dopamine, and to enhance dopamine levels after treatment with levodopa [9,10]. MAO-B inhibitors may also protect against the neurodegenerative events associated with Parkinson's disease by reducing the levels of potentially neurotoxic aldehydes and H_2O_2 which are generated as by-products in the catalytic cycle of MAO-B [11,12,13]. (*R*)-Deprenyl and rasagiline are examples of MAO-B inhibitors currently being used as adjuncts to levodopa therapy in the treatment of Parkinson's disease [14]. While these inhibitors have been widely used, their irreversible mode of inhibition may be associated with certain disadvantages. These include a slow rate of enzyme recovery after drug withdrawal and a loss of selectivity for the MAO-B isoform after repeated administration [15,16]. For these reasons, the discovery of new MAO-B inhibitors with a reversible mode of action is being pursued by various research groups.

For the design of reversible MAO inhibitors, C8-substituted caffeine analogues have been previously employed [17,18,19,20]. While caffeine is a weak MAO-B inhibitor, substitution with a variety of moieties at C8 often yields compounds that are highly potent and selective MAO-B inhibitors [21,22]. For example, a series of 8-benzyloxycaffeine analogues (**1**) (Fig. 1) has been shown to act as potent inhibitors of human MAO-B with IC_{50} values ranging from 0.068 to 1.77 µM [17]. Interestingly, the 8-benzyloxycaffeine analogues were also found to be potent MAO-A inhibitors with IC_{50} values ranging from 0.397 to 3.72 µM [17]. Modelling studies have indicated that the ability of the 8-benzyloxycaffeine analogues to also bind to the MAO-A active site may depend on the large degree of rotational freedom of the benzyloxy side chain at the carbon-oxygen ether bond [17]. More rigid C8-substituted caffeine analogues such as (*E*)-8-(3-chlorostyryl)caffeine (**2**) typically do not inhibit MAO-A [17,22,23]. Another C8 oxy substituent that leads to potent MAO-B inhibition is the 2-phenoxyethoxy moiety. In fact, 8-(2-phenoxyethoxy)caffeine (**3a**) (IC_{50} = 0.383 µM) is a more potent inhibitor of human MAO-B than is 8-benzyloxycaffeine (IC_{50} = 1.77 µM) [18]. A structure-activity relationship (SAR) study has indicated that for C8-substituted oxycaffeine analogues, a linker consisting of 4 atoms separating the caffeine and the terminal phenyl ring may be particularly suited for MAO-B inhibition [18]. Since this requirement is satisfied by the 8-(2-phenoxyethoxy)caffeine structure, this compound may be considered to be a promising lead compound for the design of highly potent MAO-B inhibitors. Of significant interest is the observation that substituted 8-oxycaffeines are reported to interact reversibly with both MAO-A and –B [17,18]. This further makes the 8-(2-phenoxyethoxy)caffeine structure relevant for the design of reversible MAO inhibitors.

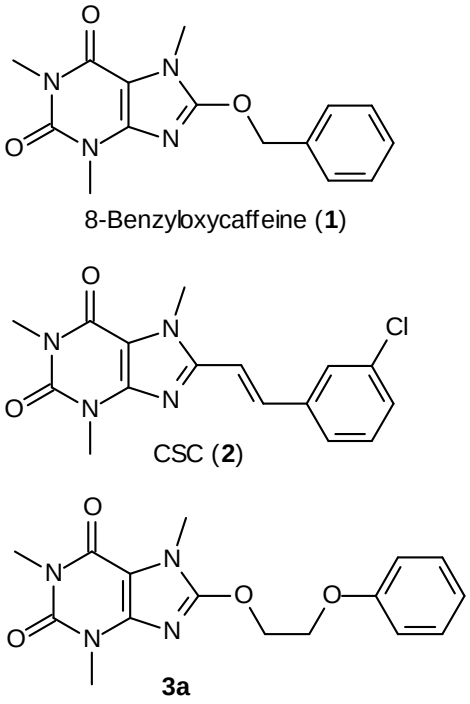

Figure 1. The structures of 8-benzyloxycaffeine (**1**), CSC (**2**) and 8-(2-phenoxyethoxy)caffeine (**3a**).

Based on these observations, in the present study the MAO-A and –B inhibition properties of a series of ten 8-(2-phenoxyethoxy)caffeine analogues (**3a**–**j**) were examined. The analogues considered, differed by substitution on the *para* position of the phenoxy ring. A previous study reported that that halogen substitution at this position leads to an enhancement of both the MAO-A and –B inhibition potencies of 8-(2-phenoxyethoxy)caffeine [18]. For the purpose of this study, quantitative structure-activity relationship (QSAR) studies were carried out in an attempt to quantify the relationship between MAO inhibitory activity of the 8-(2-phenoxyethoxy)caffeine analogues and the physicochemical properties of the substituents on the *para* position of the side chain phenoxy ring.

4.2. Results and discussion

4.2.1. Chemistry

The 8-(2-phenoxyethoxy)caffeine analogues (**3a**–**j**) were synthesized according to the protocol previously described for the synthesis of C8 substituted caffeines [24,18]. The target compounds were obtained by reacting 8-chlorocaffeine (**4**) with an appropriately substituted 2-phenoxyethanol (**5**) at high temperatures (150 ˚C) in the

presence of potassium hydroxide (Scheme 1). After recrystallization from ethanol, compounds **3a**–**j** were obtained in low to high yields (3–83%). 8-Chlorocaffeine was obtained in high yield from a reaction between chorine and a solution of caffeine in chloroform [25]. In certain instances, the 2-phenoxyethanol analogues that were required for the synthesis of **3a**–**j** were not commercially available and were thus synthesized according to literature methods [26,27]. For this purpose an appropriately substituted phenol (**6**) was reacted with 2-bromoethanol in the presence of potassium carbonate in acetone. The structures of the 8-(2-phenoxyethoxy)caffeine analogues (**3a**–**j**) were verified by mass spectrometry, ^{1}H NMR and ^{13}C NMR while the purities were estimated by chromatographic analysis.

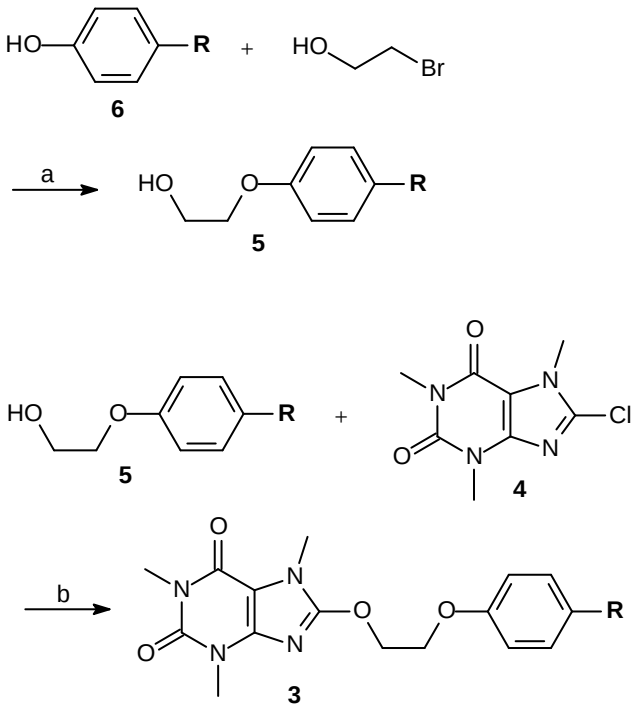

Scheme 1. Synthetic pathway to the 8-(2-phenoxyethoxy)caffeine analogues **3**. Reagents and conditions: (a) Acetone, K_2CO_3 (b) KOH, 150 ˚C.

4.2.2. Enzymology

To examine the MAO-A and –B inhibition properties of the 8-(2-phenoxyethoxy)caffeine analogues (**3a**–**j**), the commercially available recombinant human enzymes were employed and kynuramine, a MAO-A/B nonselective substrate, served as enzyme substrate. Kynuramine, a non-fluorescent compound, undergoes MAO catalyzed oxidation to yield the fluorescent compound, 4-

hydroxyquinoline, as end product. The extent to which kynuramine is oxidized to 4-hydroxyquinoline by MAO was subsequently measured via fluorescence spectrophotometry (λ_{ex} = 310 nm; λ_{em} = 400 nm) [28]. None of the inhibitors investigated in this study fluoresced at these excitation/emission wavelengths or quenched the fluorescence of 4-hydroxyquinoline at the inhibitor concentrations used. Sigmoidal dose–response curves (Fig. 2) were constructed for the inhibition of the MAO isozymes and the inhibition potencies of the test compounds were expressed as the corresponding IC_{50} values.

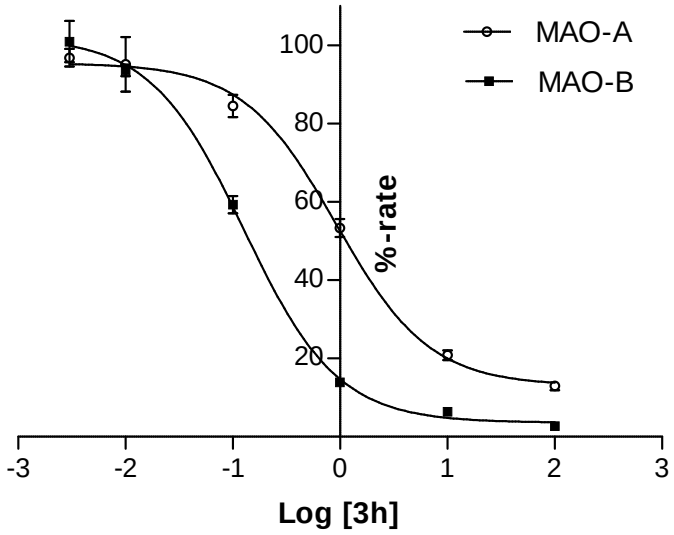

Figure 2. The recombinant human MAO-A and MAO-B catalyzed oxidation of kynuramine in the presence of various concentrations of inhibitor **3h**. The sigmoidal dose-response curves were constructed from the initial rates of kynuramine oxidation versus the logarithm of the concentration of inhibitor **3h** (expressed in nM).

The results of the MAO inhibition studies are given in Table 1. In accordance to literature, the 8-(2-phenoxyethoxy)caffeine analogues (**3a**–**j**) were found to act as inhibitors of MAO-B. The most potent inhibitor of the series was the CF_3 substituted homologue, compound **3e**, which exhibited an IC_{50} value of 0.061 μM for the inhibition of MAO-B. Compound **3e** is therefore approximately 6-fold more potent than the corresponding unsubstituted homologue **3a** (IC_{50} = 0.383 μM). The results show that a variety of substituents on C4 of the phenoxy ring lead to enhanced MAO-B inhibition compared to **3a**. These substituents are notably halogens. For example,

the Cl (IC_{50} = 0.183 µM), Br (IC_{50} = 0.166 µM), F (IC_{50} = 0.115 µM) and I (IC_{50} = 0.128 µM) substituted homologues inhibited MAO-B with potencies approximately two–threefold higher than that of the unsubstituted homologue **3a**. Non-halogen substituents on C4 of the phenoxy ring of the 8-(2-phenoxyethoxy)caffeine analogues resulted in a reduction of MAO-B inhibition potency compared to the unsubstituted homologue **3a**. For example, the CH_3 (IC_{50} = 1.41 µM) and OCH_3 (IC_{50} = 1.53 µM) substituted homologues were 3.5–4-fold weaker inhibitors of MAO-B than the unsubstituted homologue **3a**. Similarly, those homologues containing the CN (IC_{50} = 6.98 µM) and NO_2 (IC_{50} = 0.852 µM) substituents were found to be 18-fold and twofold weaker inhibitors than **3a**, respectively.

The 8-(2-phenoxyethoxy)caffeine analogues (**3a**–**j**) were also found to inhibit MAO-A. As shown by the SI values which ranged from 5–79, all of the compounds were however selective inhibitors of the MAO-B isoform. The only homologue which exhibited an IC_{50} value in the sub-micromolar range was compound **3h** which inhibited MAO-A with an IC_{50} value of 0.924 µM. With the exception of the CN substituted homologue **3i** (IC_{50} = 35.5 µM), substitution on C4 of the phenoxy ring led to an enhancement of MAO-A inhibition potency compared to the unsubstituted homologue **3a** (IC_{50} = 20.4 µM). With the exception of the F substituted homologue (IC_{50} = 9.08 µM) those homologues with halogen containing substituents (**3b**, **3c**, **3e** and **3h**) were the most potent MAO-A inhibitors of the series with IC_{50} values ranging from 0.924–2.22 µM.

Table 1. The IC_{50} values for the inhibition of recombinant human MAO-A and –B by the 8-(2-phenoxyethoxy)caffeine analogues **3a–j**.[a]

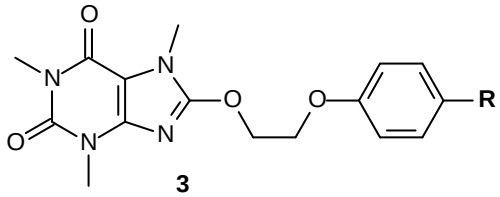

3

Compd.	**R**	IC_{50} values (μM) MAO-A	MAO-B	SI[b]
3a	-H	20.4 ± 16.5[c]	0.383 ± 0.021[c]	53
3b	-Cl	1.83 ± 0.013[c]	0.183 ± 0.005[c]	10
3c	-Br	1.65 ± 0.087[c]	0.166 ± 0.003[c]	9.9
3d	-F	9.08 ± 1.38	0.115 ± 0.004	79
3e	$-CF_3$	2.22 ± 0.068	0.061 ± 0.003	36
3f	$-CH_3$	13.4 ± 0.549	1.41 ± 0.068	9.5
3g	$-OCH_3$	7.57 ± 0.187	1.53 ± 0.185	5.0
3h	-I	0.924 ± 0.031	0.128 ± 0.013	7.2
3i	-CN	35.5 ± 3.04	6.98 ± 0.433	5.1
3j	$-NO_2$	4.92 ± 0.286	0.852 ± 0.007	5.8

[a] Values are expressed as the mean ± SD of triplicate determinations.

[b] The selectivity index (SI) is the selectivity for the MAO-B isoform and is given as the ratio of IC_{50}(MAO-A/IC_{50}(MAO-B).

[c] Values obtained from literature [18].

4.2.3. Reversibility of inhibition

As mentioned in the introduction, literature reports that 8-oxycaffeines interact reversibly with both MAO-A and –B [17,18]. To verify that the most potent MAO-A inhibitor of the present series, compound **3h**, and the most potent MAO-B inhibitor, compound **3e**, are reversible inhibitors, the recoveries of the enzymatic activities after dilution of enzyme-inhibitor complexes were evaluated. The MAO enzymes were preincubated with compounds **3h** and **3e** at concentrations of 10 × IC_{50} and 100 × IC_{50} for 30 min and then diluted to 0.1 × IC_{50} and 1 × IC_{50}, respectively. The results are presented in Fig. 3 and show that after diluting **3h** and **3e** to concentrations equal to 0.1 × IC_{50}, the MAO-A and –B activities were recovered to levels of 97% and 65%

of the control values, respectively. This behavior is consistent with a reversible interaction of **3h** with MAO-A and **3e** with MAO-B.

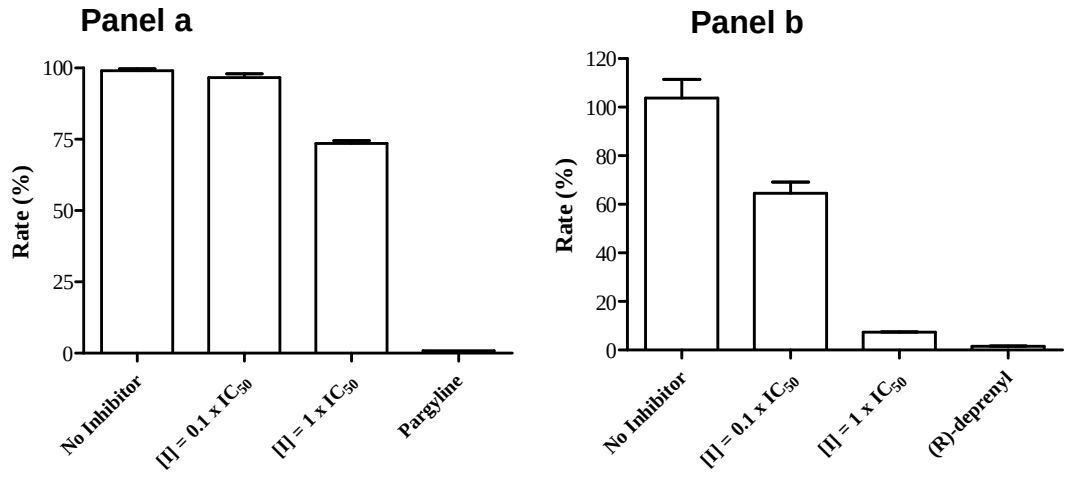

Figure 3. Reversibility of inhibition of MAO-A and –B by compounds **3h** and **3e**. (a) MAO-A was preincubated with **3h** and (b) MAO-B was preincubated with **3e**, at 10 × IC_{50} and 100 × IC_{50} for 30 min and then diluted to 0.1 × IC_{50} and 1 × IC_{50}, respectively. The residual enzyme activities were subsequently measured.

4.2.4. QSAR studies

In an attempt to quantify the relationships between the MAO-A and –B inhibition activities of the 8-(2-phenoxyethoxy)caffeine analogues and the physicochemical properties of the substituents on C4 of the phenoxy ring, a Hansch-type SAR study was carried out. For this purpose, the physicochemical properties of the substituents were described by 5 classical parameters. The Taft steric parameter (E_s) [29] and Van der Waals volume (V_w) [30] served as descriptors of size and bulkiness while the lipophilicities of the substituents were described by the Hansch constant (π) [29]. The electronic properties of the C4 substituents were described by the classical Hammett constant (σ_p) and the Swain–Lupton constant (*F*) [29]. The values of the substituent descriptors were obtained from standard compilations [29,30]. Compounds **3a**–**h** were used for the QSAR study and the results of the statistical analysis for MAO-A and –B are shown in Tables 2 and 3, respectively. Compounds **3i**–**j**, the CN and NO_2 substituted homologues, were excluded for the QSAR study since meaningful models could not be obtained with the inhibition data of these compounds included in the analyses. This behavior is in accordance with literature, which reports that in similar

QSAR studies with MAO substrates, the *p*-NO_2 groups of *p*-NO_2-phenethylamine [31] and *p*-NO_2-benzylamine [32] result in anomalous fits, and these compounds were also excluded from the regression analyses in these studies. The current study shows that the CN functional group produces similar anomalous behavior, at least for the binding of 8-(2-phenoxyethoxy)caffeine analogues to the MAO enzymes. It has been suggested that additional interactions, such as hydrogen bonding, between these functional groups and the MAO active sites may be responsible for this behavior [31].

Table 2. Correlations of the recombinant human MAO-A inhibition potencies ($logIC_{50}$) of 8-(2-phenoxyethoxy)caffeine analogues **3a**–**h** with steric, electronic and hydrophobic descriptors of the substituents at C4 of the phenoxy ring.[a]

Parameter	Slope	*y*-intercept	R^2	F	Significance[b]
σ_p	–1.29 ± 0.59	0.76 ± 0.15	0.44	4.79	0.071
F	–2.00 ± 0.67	1.24 ± 0.24	0.60	8.94	0.024
V_w	–0.62 ± 0.23	1.28 ± 0.27	0.54	7.16	0.037
π	–0.97 ± 0.23	1.15 ± 0.16	0.74	17.0	0.006
E_s	0.42 ± 0.22	1.07 ± 0.27	0.39	3.84	0.098
σ_p + π	–0.3 ± 0.59	1.11 ± 0.18	0.75	7.59	0.634
	–0.85 ± 0.34				0.055
σ_p + V_w	–1.16 ± 0.28	1.34 ± 0.14	0.90	22.2	0.009
	–0.57 ± 0.12				0.005
π + *F*	–0.72 ± 0.16	1.39 ± 0.12	0.92	30.0	0.006
	–1.25 ± 0.36				0.018

[a] The logarithm of the IC_{50} values (expressed in μM) was used for the linear regression analyses.

[b] The significance is the fractional probability that the coefficient of the added variable is zero.

Table 3. Correlations of the recombinant human MAO-B inhibition potencies ($logIC_{50}$) of 8-(2-phenoxyethoxy)caffeine analogues **3a**–**h** with steric, electronic and hydrophobic descriptors of the substituents at C4 of the phenox ring.[a]

Parameter	Slope	*y*-intercept	R^2	F	Significance[b]
σ_p	–1.83 ± 0.34	–0.40 ± 0.088	0.83	29.0	0.002
F	–1.81 ± 0.81	–0.035 ± 0.29	0.45	4.92	0.068
V_w	0.015 ± 0.36	–0.60 ± 0.42	0.0003	0.002	0.968
Π	–0.63 ± 0.402	–0.25 ± 0.27	0.29	2.44	0.169
E_s	0.32 ± 0.26	–0.25 ± 0.32	0.20	1.54	0.260
$\sigma_p + \pi$	–2.03 ± 0.49	–0.47 ± 0.15	0.84	13.2	0.009
	0.17 ± 0.28				0.569
$\sigma_p + V_w$	–1.85 ± 0.36	–0.50 ± 0.36	0.84	13.2	0.004
	0.10 ± 0.16				0.570

[a] The logarithm of the IC_{50} values (expressed in μM) was used for the linear regression analyses.

[b] The significance is the fractional probability that the coefficient of the added variable is zero.

Analysis of the results of the MAO-A inhibition studies revealed that the best one parameter correlation existed between $logIC_{50}$ and π. The R^2 value was 0.74 while the statistical F value was 17.0 (F_{max} = 20.62). Addition of a second parameter yielded significantly improved correlations. The most significant correlation was a two parameter fit of $logIC_{50}$ versus the Swain–Lupton constant (*F*) and π. The R^2 value of this correlation was 0.92 while the statistical F value was 30.0. Since the statistical F value is higher than the F_{max} value (20.85) for 95% significance (a higher F value indicates a better fit), this correlation may be considered statistically significant [33]. For this correlation, the probabilities that π and *F* are zero are 0.6% and 1.8%, respectively. Therefore, the best mathematical description of the MAO-A inhibition potencies ($logIC_{50}$) of the 8-(2-phenoxyethoxy)caffeine analogues (**3a**–**h**) is (Fig. 4):

$$LogIC_{50} = -0.72(\pm 0.16)\pi - 1.25(\pm 0.36)F - 1.39(\pm 0.12)$$
$$(R^2 = 0.92 \text{ and } F = 30.0) \quad (1)$$

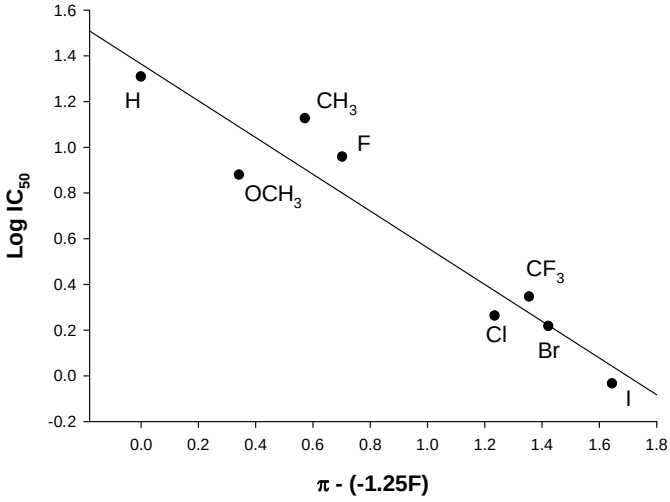

Figure 4. Correlations of the logIC_{50} values for the inhibition of recombinant human MAO-A by **3a**–**h** with the Hansch constant (π) of the substituents at C4 of the phenoxy ring. The π values were adjusted by the contribution of the Swain-Lupon constant (*F*) as indicated on the x-axis title. The linear regression line is a representation of equation 1 with a correlation coefficient of 0.92.

Other two parameter fits also yielded meaningful correlations. A two parameter model of logIC_{50} versus σ_p and π resulted in a R^2 value of 0.75 with a statistical F value of 7.59 (F_{max} = 20.85). Similarly, a two parameter fit of logIC_{50} versus σ_p and V_w resulted in a R^2 of 0.90 and a statistical F value of 22.2 (F_{max} = 20.85). The negative signs observed for the π parameter coefficients of these models suggest that the potency of MAO-A inhibition by 8-(2-phenoxyethoxy)caffeine analogues may be enhanced by substituents on C4 of the 2-phenoxy ring with a high degree of lipophilicity. The negative signs of the *F* and σ_p parameter coefficients of these models suggest that electron withdrawing substituents at C4 of the phenoxy ring of the 8-(2-phenoxyethoxy)caffeine analogues may enhance inhibition potency. Since the Van der Waals volume (V_w) is a descriptor of bulkiness, a negative correlation ($-0.57V_w$) is an indication that more bulky substituents may result in more potent inhibition of MAO-A.

Analysis of the results of the MAO-B inhibition studies yielded a significant single parameter correlation between the LogIC_{50} values the Hammett constant (σ_p) with a

R^2 value of 0.83. The statistical F value for the correlation was found to be 29.0 (F_{max} 20.62). The inclusion of an additional parameter resulted in slightly improved correlations. A two parameter fit of $logIC_{50}$ versus σ_p and V_w resulted in a R^2 value of 0.84 and a statistical F value of 13.2 (F_{max} 20.85). For this correlation the probability that σ_p and V_w are zero is 0.4% and 57%, respectively. A two parameter fit with σ_p and the Hansch constant (π) also resulted in a reasonable correlation with a R^2 value of 0.84 and a statistical F value of 13.2. The probability that σ_p and π are zero is 0.9% and 57%, respectively. This suggests that the contribution of V_w and π to these correlations may be neglected. The best mathematical description for the MAO-B inhibition potencies ($logIC_{50}$) of the 8-(2-phenoxyethoxy)caffeine analogues (**3a**–**h**) is therefore (Fig. 5):

$$LogIC_{50} = -1.83(\pm 0.34)\sigma_p - 0.40(\pm 0.088)$$
$$(R^2 = 0.83 \text{ and } F = 29.0) \qquad (2)$$

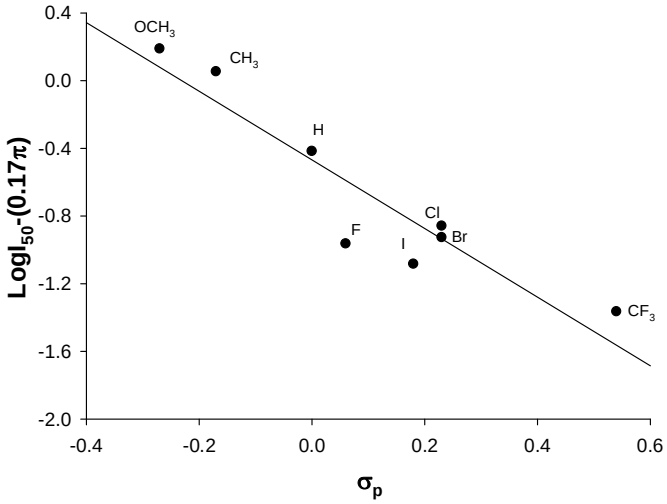

Figure 5. Correlations of the $logIC_{50}$ values for the inhibition of recombinant human MAO-B by **3a**–**h** with the Hammet electronic parameter (σ_p) of the substituents at C4 of the phenoxy ring. The $logIC_{50}$ values were adjusted by the contribution of the Van der Waals volume (V_w) as indicated on the y-axis title. The linear regression line is a representation of equation 2 with a correlation coefficient of 0.84.

The negative correlation observed between $logIC_{50}$ and σ_p ($-1.83\sigma_p$) is an indication that substitution at C4 of the phenoxy ring with electron withdrawing groups may enhance the MAO-B inhibition potencies of the 8-(2-phenoxyethoxy)caffeine analogues. This result is in accordance to similar studies with oxycaffeine analogues.

For example, for the inhibition of baboon liver MAO-B and recombinant human MAO-B by a series of 8-benzyloxycaffeine analogues, the inhibition potencies ($logIC_{50}$) exhibited a negative correlation with σ_p (–1.23π) [17]. The finding that Vw and π do not significantly contribute to correlations of $logIC_{50}$ is dissimilar to the QSAR results obtained with MAO-A, where a negative correlations with both V_w and π were observed.

4.2.5. Molecular modeling

To provide additional insight into the results obtained with the QSAR study, a selected 8-(2-phenoxyethoxy)caffeine analogue, compound **3e**, was docked into active site cavity models of MAO-A and –B. Compound **3e** was selected as representative compound since it was found to be the most potent MAO-B inhibitor among the series of 8-(2-phenoxyethoxy)caffeine analogues. The preparation of the models and the docking experiments were carried out with the Windows based Discovery Studio 3.1 modeling software (Accelrys) [34] according to a previously reported protocol [35,18]. As enzyme models, the crystallographic structures of human MAO-A complexed with harmine (PDB entry: 2Z5X) [36] and human MAO-B in complex with 7-(3-chlorobenzyloxy)-4-formylcoumarin (PDB entry: 2V60) [37] were selected. For the purpose of the docking study, the CDOCKER module of Discovery Studio 3.1 was employed (see Experimental section). This docking protocol has been shown to be suitable for predicting binding orientations of ligands to the active sites of MAO-A and –B [35].

The best ranked binding orientation of **3e** in the MAO-B active site is shown in Fig. 6. The 10 highest ranked solutions display highly similar binding orientations with RMSD values of less than 1.4 Å from the position of the highest ranked orientation. The caffeine ring of **3e** is placed within the substrate cavity of the enzyme, in front of the isoalloxazine ring of the FAD cofactor and approximately parallel to the phenolic side chains of the Tyr-398 and Tyr-435. This region is considered to be the polar part of the MAO-B active site. The orientation of the caffeine ring of **3e** is, for the most part, guided by the flat shape of the substrate cavity of MAO-B [38,18]. The carbonyl oxygen at C6 of the caffeine ring is within hydrogen bond interaction distance to an active site water molecule (HOH 1159). Since **3e** binds relatively close to the FAD cofactor, a π–π interaction is predicted to occur between the caffeine ring and the

aromatic ring of Tyr-398. The C8 substituent of **3e** project towards the entrance cavity of MAO-B and the phenoxy ring is placed well within the entrance cavity. Since the entrance cavity is lined by the side chains of hydrophobic amino acid residues (Phe-103, Trp-119, Leu-164, Leu-167, Phe-168 and Ile-316), the C8 substituents are stabilized principally by Van der Waals interactions within the entrance cavity [39]. Of note is a potential π–π interaction between the phenyl ring of the inhibitor and the aromatic ring of Tyr-326. This binding orientation and predicted interactions are similar to those previously found, via docking experiments, for the binding of 8-benzyloxycaffeine (**1**) to MAO-B [17]. It should be noted that the residue Ile-199, which acts as a 'gate' between the substrate and entrance cavities, should be in an open conformation. This allows for the fusion of the two cavities into a single space large enough for larger ligands to bind to MAO-B. The ability of the side chain of Ile-199 to rotate from the active site cavity into an alternate conformation is a unique feature of the MAO-B active site and is thought to be responsible for the observed selective binding of relatively large inhibitors to MAO-B compared to MAO-A [40].

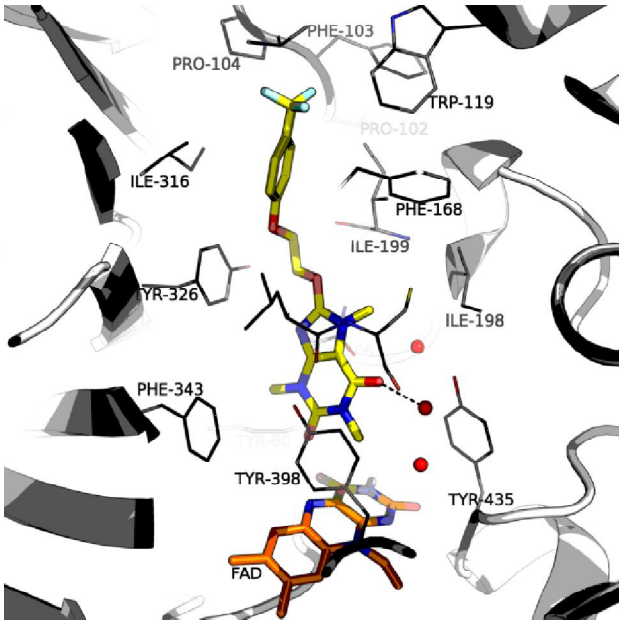

Figure 6. The highest ranked docking solution of compound **3e** within an active site model of MAO-B.

The best ranked binding orientation of **3e** within the MAO-A active site is shown in Fig. 7. The caffeine ring of compound **3e** exhibits a similar binding orientation in MAO-A compared to the predicted orientation in MAO-B. The caffeine moiety is bound in proximity to the FAD cofactor with the carbonyl oxygen at C2 of the caffeine ring placed within hydrogen bond interaction distance to the phenolic hydrogen of Tyr-444. The C8 oxy side chain extends towards the entrance of the active site cavity and, in contrast to the observed conformation in MAO-B, is bent by a relatively large degree from the plane of the caffeine ring. MAO-A is reported to have a smaller active site cavity than MAO-B with the benzyl side chain of residue Phe-208 protruding into the cavity [36,41]. To avoid structural overlap with Phe-208, larger inhibitors, such as **3e**, bind in this bent conformation. In the MAO-B active site, the residue that corresponds to Phe-208 in MAO-A, is Ile-199. The small volume of the side chain of Ile-199 allows the side chain of this residue to partially rotate out of the active site, allowing sufficient space for larger inhibitors to bind in an extended conformation [40]. The flexibility of inhibitor **3e** may be attributed to rotation around the C8 carbon-oxygen ether bond. As mentioned in the Introduction, this relatively large degree of rotational freedom is, to a large degree, responsible for the ability of the 8-(2-phenoxyethoxy)caffeine analogues to bind to MAO-A. An interesting observation is that **3e** is predicted to undergo two π–π interactions with the active site of MAO-B – one with Tyr-398 in the substrate cavity and one with Tyr-326 at the boundary between the substrate and entrance cavities. Even though MAO-A contains an aromatic amino acid residue (Tyr-407) at the analogous position to Tyr-398 in MAO-B, **3e** is predicted not to undergo π–π interactions with MAO-A. This suggests that, in MAO-B, **3e** may adopt an optimal orientation which allows for these π–π interactions to occur, while in MAO-A such an orientation is not permitted. These differential binding orientations leads to different interaction modes and may, at least in part, explain the selectivities of the 8-(2-phenoxyethoxy)caffeine analogue for MAO-B.

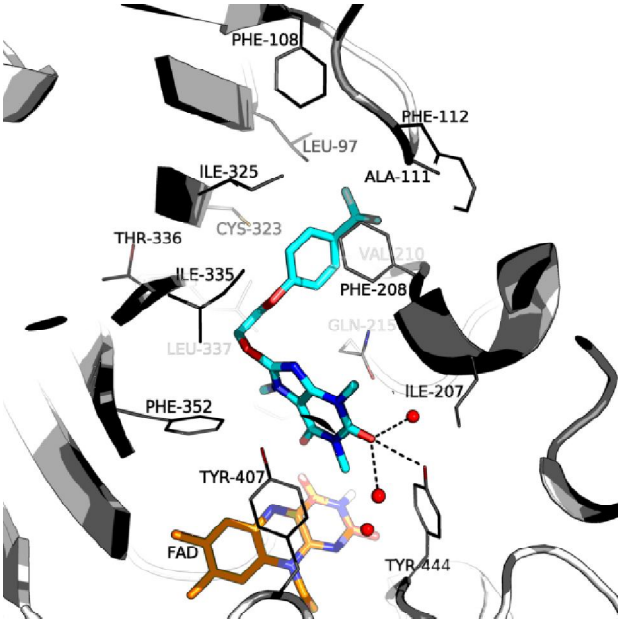

Figure 7. The highest ranked docking solution of compound **3e** within an active site model of MAO-A.

4.3. Conclusion

Based on a previous report that 8-(2-phenoxyethoxy)caffeine (**3a**) is potent MAO-B inhibitor and potentially suitable lead for the design of reversible MAO-B inhibitors, the present study investigates the SAR for the inhibition of human MAO-A and –B by a series of 8-(2-phenoxyethoxy)caffeine analogues containing different substiutuents on the *para* position of the phenoxy ring [18]. The results document that, compared to **3a**, substitution with halogen containing groups leads to an enhancement in MAO-B inhibition potency while non-halogen substituents reduce the MAO-B inhibition potencies of the 8-(2-phenoxyethoxy)caffeine analogues. Based on the results of the QSAR study, which demonstrates a negative correlation between the MAO-B inhibition potencies and the Hammett constant ($-1.83\sigma_p$), electron withdrawing functional groups on C4 of the phenoxy ring are expected to enhance the inhibition potency of 8-(2-phenoxyethoxy)caffeine. It may therefore be concluded the electron withdrawing properties of the halogen containing substituents are, to a large degree, responsible for the observed enhancement of MAO-B inhibition potencies of the 8-(2-phenoxyethoxy)caffeine analogues. Conversely, those substituents that may be considered electron releasing (CH_3 and OCH_3) reduce the MAO-B inhibition potencies of the 8-(2-phenoxyethoxy)caffeine analogues. This finding of the QSAR

study is in accordance to similar studies reported in literature. For example, for the MAO-B by a series of 8-benzyloxycaffeine analogues, the inhibition potencies exhibited a negative correlation with the Hammett constant of substituents on the benzyloxy ring [17]. The results of the QSAR study suggests there exists no correlation between the MAO-B inhibition potencies of the 8-(2-phenoxyethoxy)caffeine analogues and the Hansch constant (π). This finding is in contrast to a previous study which demonstrated that a series of 8-benzyloxycaffeine analogues exhibits a negative correlation with π [17]. This suggested that the MAO-B inhibition potencies of 8-benzyloxycaffeines may be enhanced with substitution of more lipophilic functional groups on the benzyloxy ring. Since the modeling studies suggest that the phenoxy ring of the present series binds within the entrance cavity of the MAO-B active site, which is considered to be a mostly hydrophobic space, it may be expected that C4 substituents with enhanced lipophilicity may interact more favorably via Van der Waals interactions in this region and thus lead to improved MAO-B inhibition. The QSAR study, however, finds that no correlation exists between the MAO-B inhibition potencies and the Hansch constant (π). This indicates that the phenoxyethoxy side chain binds in an optimal position in the MAO-B entrance cavity and no further increase in lipophilicity will improve interaction with this cavity. This result is further support for the proposal of a previous study, which has shown that for C8-substituted oxycaffeine analogues, a linker consisting of 4 atoms separating the caffeine and the terminal phenyl ring may be optimal for MAO-B inhibition [18]. For example, the oxycaffeine homologue substituted with a benzyloxyethoxy side chain (IC_{50} = 3.77 µM) contains a linker which consists of 5 atoms and is, as a result, approximately 9 fold less potent as an MAO-B inhibitor than **3a** [18]. In contrast to a linker consisting of 4 atoms which places the phenyl ring in an optimal position in the entrance cavity, a linker consisting of 2 atoms (such as found in 8-benzyloxycaffeine, IC_{50} = 1.77 µM) places the phenyl ring in a less than optimal position for interaction with the MAO-B entrance cavity, and the addition of lipophilic substituents to the phenyl ring is required to improve interaction.

The 8-(2-phenoxyethoxy)caffeine analogues (**3a**–**j**) were also found to be inhibitors of human MAO-A. With the exception of the CN substituted homologue **3i**, substitution on C4 of the phenoxy ring resulted in an enhancement of MAO-A inhibition potency compared to the unsubstituted homologue **3a**. The QSAR study suggests that this

enhancement is dependent on a combination of properties of the C4 substituent. A negative correlation between the MAO-A inhibition potencies and the Swain–Lupton constant (–1.25*F*), explains the observation that electron withdrawing functional groups on C4 of the phenoxy ring, such as the halogen containing groups, enhance the inhibition potency of 8-(2-phenoxyethoxy)caffeine. The highly significant negative correlation between the MAO-A inhibition potencies of the 8-(2-phenoxyethoxy)caffeine analogues and the Hansch constant (–0.72π) suggests that C4 substituents with high degrees of lipophilicities may enhance MAO-A inhibition potency. This explains the observation that electron releasing substituents (CH_3 and OCH_3) with relatively high degrees of lipophilicities may also enhance the MAO-A inhibition potency of 8-(2-phenoxyethoxy)caffeine. The molecular docking studies suggest that the phenoxy ring binds towards the entrance of the MAO-A active site cavity. In this region, lipophilic C4 substituents may undergo favourable Van der Waals interactions and thus lead to enhanced MAO-A inhibition. Interestingly, the QSAR study suggests that a negative correlation between the MAO-A inhibition potencies and the Van der Waals volume (–0.57V_w) may exist. From this result it may be expected that substitution at C4 of the phenoxy ring with relatively larger substituents would be more favourable for binding of the 8-(2-phenoxyethoxy)caffeine analogues to MAO-A. This result is dissimilar to that observed for the QSAR study with MAO-B which found no correlation with V_w. Although the MAO-A active site is reported to be smaller than the MAO-B active site, this result suggests that, in contrast to their binding modes in MAO-B, the 8-(2-phenoxyethoxy)caffeine analogues do not completely fill the MAO-A active site [36]. The modeling studies predict that the inhibitors bind in a bent conformation in MAO-A which may allow for the availability additional space in the active site. With the availability of additional space in the MAO-A active site, larger C4 substituents may be accommodated.

4.4. Experimental

4.4.1. Materials and instrumentation

All starting materials, unless otherwise noted, were acquired from Sigma–Aldrich and were used without further purification. Proton (^1H) and carbon (^{13}C) NMR spectra were recorded in $CDCl_3$ and DMSO-d_6 with a Bruker Avance III 600 spectrometer at

frequencies of 600 MHz and 150 MHz, respectively. Chemical shifts are reported in parts per million (δ) downfield from the signal of tetramethylsilane added to the deuterated solvent. Spin multiplicities are given as s (singlet), d (doublet), t (triplet) or m (multiplet). Direct insertion electron impact ionization mass spectra (EIMS) and high resolution mass spectra (HRMS) were obtained on a DFS high resolution magnetic sector mass spectrometer (Thermo Electron Corporation). Melting points (mp) were measured with a Buchi M-545 melting point apparatus and are uncorrected. The purities of the synthesized compounds were estimated by HPLC analyses which were carried out with an Agilent 1100 HPLC system equipped with a quaternary pump and an Agilent 1100 series diode array detector (see Supplementary Material). HPLC grade acetonitrile (Merck) and Milli-Q water (Millipore) was used for these chromatographic analyses. Fluorescence spectrophotometry was conducted with a Varian Cary Eclipse fluorescence spectrophotometer. Microsomes from insect cells containing recombinant MAO-A and –B (5 mg/mL) and kynuramine·2HBr were obtained from Sigma–Aldrich. 8-Chlorocaffeine (**4**) was prepared according to a previously reported procedure [25] by reaction of caffeine with chlorine in chloroform. The melting point (188 ˚C) as well as the NMR spectra correlated to the corresponding published values [25,42]. The 2-phenoxyethanol analogues (**5**) which were required as reactants for the synthesis of **3** were prepared by reacting the appropriately substituted phenol (**6**) with bromoethanol in the presence of acetone and potassium carbonate [26,27].

*4.4.2. Procedures for the synthesis of the 8-(2-phenoxyethoxy)caffeine analogues (**3**)*

For the synthesis of compounds **3a**–**d** a method described in literature was followed with minor modifications [43]. Metallic sodium (1.5 mmol) and the appropriately substituted phenoxyethanol analogue (**5**, 21 mmol) were allowed to react at room temperature. Following consumption of the sodium, 8-chlorocaffeine (**4**, 1.5 mmol) was added and the resulting mixture was stirred for 6 hours at 150 °C. The reaction was cooled to room temperature and the 8-(2-phenoxyethoxy)caffeine analogue was recrystallized (at 4 °C) after the addition of ethanol (10–20 mL) to the reaction mixture. The melting points and structure characterizations of compounds **3a**–**c** have been previously reported [18]. The physical data of **3d** are cited below.

The 8-(2-phenoxyethoxy)caffeine analogues **3e–j** were synthesized according the literature procedure by Baumann et al. [24] Potassium hydroxide (2 mmol) was dissolved in 1 mL distilled water and the appropriately substituted 2-phenoxyethanol analogue (1.85 mmol) was added to yield a solution. 8-Chlorocaffeine (**4**, 1.5 mmol) was added and the resulting reaction mixture was stirred at 150 °C for 6 hours. The reaction was cooled to room temperature and ethanol (10 mL) was added. The resulting solution was allowed to recrystallize (at 4 °C).

*4.4.2.1. 8-[2-(4-Fluorophenoxy)ethoxy]caffeine (**3d**)*

The title compound was prepared from 8-chlorocaffeine (**4**) and 2-(4-fluorophenoxy)ethanol. (63%) cream colored solid: mp 177 ºC (from ethanol). ^{1}H NMR (600 MHz, $CDCl_3$, Me_4Si) 3.37 (3H, s, CH_3), 3.49 (3H, s, CH_3), 3.68 (3H, s, CH_3), 4.29 (2H, t, CH_2, J = 4.52 Hz), 4.77 (2H, t, CH_2, J = 4.52 Hz), 6.85 (2H, m, phenyl), 6.97 (2H, m, phenyl); ^{13}C NMR (150 MHz, $CDCl_3$, Me_4Si) 27.76, 29.75, 29.90, 66.48, 69.20, 103.62, 115.69 (d), 115.90, 116.06, 146.07, 151.67, 154.45, 154.83, 155.27; HRMS *m/z*: calcd for $C_{16}H_{17}FN_4O_4$, 348.1234, found 348.12144; Purity (HPLC): 98%.

*4.4.2.2. 8-{2-[4-(Trifluoromethyl)phenoxy]ethoxy}caffeine (**3e**)*

The title compound was prepared from 8-chlorocaffeine (**4**) and 2-[4-(trifluoromethyl)phenoxy]ethanol. (3%) white solid: mp 130 ºC (from ethanol). ^{1}H NMR (600 MHz, $CDCl_3$, Me_4Si) 3.36 (3H, s, CH_3), 3.49 (3H, s, CH_3), 3.67 (3H, s, CH_3), 4.37 (2H, t, CH_2, J = 3.39 Hz), 4.81 (2H, t, CH_2, J = 3.01 Hz), 6.97 (2H, d, phenyl, J = 7.91 Hz), 7.54 (2H, d, phenyl, J = 7.91 Hz); ^{13}C NMR (150 MHz, $CDCl_3$, M_4Si) 27.75, 29.74, 29.90, 65.89, 68.86, 103.65, 114.52, 125.14 (q), 127.01, 127.03, 146.03, 151.65, 154.83, 155.16, 160.71; HRMS *m/z*: calcd for $C_{17}H_{17}F_3N_4O_4$, 398.1202, found 398.11982; Purity (HPLC): 93%.

*4.4.2.3. 8-[2-(4-Methylphenoxy)ethoxy]caffeine (**3f**)*

The title compound was prepared from 8-chlorocaffeine (**4**) and 2-(4-methylphenoxy)ethanol). (83%) white solid: mp 144 ºC (from ethanol). ^{1}H NMR (600 MHz, $CDCl_3$, Me_4Si) 2.27 (3H, s, CH_3–phenyl), 3.49 (3H, s, CH_3), 3.64 (3H, s, CH_3), 3.67 (3H, s, CH_3), 4.3 (2H, t, CH_2, J = 4.52 Hz), 4.77 (2H, t, CH_2, J = 4.52 Hz), 6.81 (2H, d, phenyl, J = 8.69 Hz), 7.07 (2H, d, phenyl, J = 8.28 Hz); ^{13}C NMR (150 MHz,

$CDCl_3$, Me_4Si) 20.46, 27.75, 29.75, 29.89, 65.92, 69.37, 103.58, 114.51, 130.01, 130.74, 146.11, 151.68, 154.83, 155.37, 156.21; HRMS *m/z*: calcd for $C_{17}H_{20}N_4O_4$, 344.1485, found 344.14799; Purity (HPLC): 98%.

*4.4.2.4. 8-[2-(4-Methoxyphenoxy)ethoxy]caffeine (**3g**)*

The title compound was prepared from 8-chlorocaffeine (**4**) and 2-(4-methoxyphenoxy)ethanol. (5%) sand colored solid: mp 138 ºC (from ethanol). ^1H NMR (600 MHz, $CDCl_3$, Me_4Si) 3.36 (3H, s, CH_3), 3.49 (3H, s, CH_3), 3.67 (3H, s, CH_3), 3.75 (3H, s, OCH_3), 4.27 (2H, t, CH_2, J = 4.52 Hz), 4.76 (2H, t, CH_2, J = 4.52 Hz), 6.83 (2H, m, phenyl), 6.84 (2H, m, phenyl); ^{13}C NMR (150 MHz, $CDCl_3$, Me_4Si) 27.73, 29.73, 29.88, 55.70, 66.59, 69.40, 103.56, 114.69, 115.74, 146.09, 151.66, 152.43, 154.31, 154.81, 155.35; HRMS *m/z*: calcd for $C_{17}H_{20}N_4O_5$, 360.1434, found 360.14343; Purity (HPLC): 98%.

*4.4.2.5. 8-[2-(4-Iodophenoxy)ethoxy]caffeine (**3h**)*

The title compound was prepared from 8-chlorocaffeine (**4**) and 2-(4-iodophenoxy)ethanol. (4%) white solid: mp 160 ºC (from ethanol). ^1H NMR (600 MHz, $CDCl_3$, Me_4Si) 3.36 (3H, s, CH_3), 3.49 (3H, s, CH_3), 3.67 (3H, s, CH_3), 4.29 (2H, m, CH_2), 4.77 (2H, m, CH_2), 6.69 (2H, d, phenyl, J = 7.91 Hz), 7.55 (2H, d, phenyl, J = 7.53 Hz); ^{13}C NMR (150 MHz, $CDCl_3$, Me_4Si) 27.74, 29.74, 29.90, 65.85, 68.98, 83.54, 103.61, 116.95, 138.35, 146.03, 151.64, 154.81, 155.19, 158.20; HRMS *m/z*: calcd for $C_{16}H_{17}IN_4O_4$, 456.0294, found 456.02678; Purity (HPLC): 98%.

*4.4.2.6. 8-[2-(4-Cyanophenoxy)ethoxy]caffeine (**3i**)*

The title compound was prepared from 8-chlorocaffeine (**4**) and 2-(4-cyanophenoxy)ethanol. (8%) white solid: mp >300 ºC (from ethanol). ^1H NMR (600 MHz, DMSO-d_6, Me_4Si) 3.18 (3H, s, CH_3), 3.35 (3H, s, CH_3), 3.56 (3H, s, CH_3), 4.43 (2H, m, CH_2), 4.77 (2H, m, CH_2), 7.02 (2H, d, phenyl, J = 9.04 Hz), 7.83 (2H, d, phenyl, J = 8.66 Hz); ^{13}C NMR (150 MHz, DMSO-d_6, Me_4Si) 27.38, 29.50, 29.64, 65.89, 69.43, 102.69, 114.03, 126.89, 129.39, 145.53, 150.87, 153.85, 154.98, 160.47, 167.31; HRMS *m/z*: calcd for $C_{17}H_{17}N_5O_4$, 355.1281, found 355.12751; Purity (HPLC): 88%.

*4.4.2.7. 8-[2-(4-Nitrophenoxy)ethoxy]caffeine (**3j**)*

The title compound was prepared from 8-chlorocaffeine (**4**) and 2-(4-nitrophenoxy)ethanol. (63%) white solid: mp 178 ºC (from ethanol). ^{1}H NMR (600 MHz, $CDCl_3$, Me_4Si) 3.35 (3H, s, CH_3), 3.48 (3H, s, CH_3), 3.68 (3H, s, CH_3), 4.43 (2H, t, CH_2, J = 4.52 Hz), 4.83 (2H, t, CH_2, J = 4.52 Hz), 6.98 (2H, d, phenyl, J = 9.41 Hz), 8.19 (2H, d, phenyl, J = 9.04 Hz); ^{13}C NMR (150 MHz, $CDCl_3$, Me_4Si) 27.72, 29.72, 29.91, 66.35, 68.55, 103.64, 114.48, 125.93, 141.92, 145.93, 151.58, 154.76, 154.98, 163.17; HRMS *m/z*: calcd for $C_{16}H_{17}N_5O_6$, 375.1179, found 375.11723; Purity (HPLC): 98%.

4.4.3. IC_{50} determinations

Microsomes from baculovirus infected insect cells expressing recombinant human MAO-A or –B (5 mg/mL) were pre-aliquoted and stored at –70 °C. All enzymatic reactions were carried out in 2 mL microcentrifuge tubes in potassium phosphate buffer (100 mM, pH 7.4) which were made isotonic with KCl (20.2 mM). The final volumes of the reactions were 500 µL and contained MAO-A or MAO-B (0.0075 mg/mL) and various concentrations of the test inhibitor (0.003–100 µM). Stock solutions of the test inhibitors were prepared in DMSO and added to the reactions to yield a final concentration of 4% (v/v) DMSO. Kynuramine at concentrations of 45 µM and 30 µM served as substrate for MAO-A and –B, respectively. The reactions were incubated in a water bath at 37 °C for 20 min and terminated with the addition of 400 µL NaOH (2 N). Distilled water (1000 µL) was subsequently added to each reaction, and the concentrations of the MAO generated 4-hydroxyquinoline in the reactions were measured by fluorescence spectrophotometry (λ_{ex} = 310 nm, λ_{em} = 400 nm) [39]. A linear calibration curve was constructed from solutions of authentic 4-hydroxyquinoline (0.047–1.5 µM) dissolved in potassium phosphate buffer (100 mM, pH 7.4) which contained 4% DMSO as co-solvent. To each standard 400 µL NaOH (2 N) and 1000 µL distilled water was added. IC_{50} values were determined by plotting the initial rate of kynuramine oxidation versus the logarithm of the inhibitor concentration to obtain a sigmoidal dose–response curve. For each curve, 6 different inhibitor concentrations spanning at least 3 orders of a magnitude were used. These data were fitted to the one site competition model incorporated into the Prism 5 software package (GraphPad). All experiments were carried out in triplicate and the IC_{50} values are expressed as mean ± standard deviation (SD) [17].

4.4.4. Recovery of enzyme activity after dilution

Compound **3h** at a concentration equal to 10 × IC_{50} (9.24 µM) and 100 × IC_{50} (92.4 µM) for the inhibition of MAO-A was preincubated with recombinant human MAO-A (0.75 mg/ml) was for 30 min at 37 ºC in potassium phosphate buffer (100 mM, pH 7.4, made isotonic with KCl). Compound **3e** was similarly preincubated with recombinant human MAO-B (0.75 mg/ml) at a concentration equal to 10 × IC_{50} (0.61 µM) and 100 × IC_{50} (6.1 µM). Control incubations were conducted in the absence of inhibitor and DMSO (4%) was added as co-solvent to all preincubations. The reactions were diluted 100-fold with the addition of kynuramine to yield final concentrations of compounds **3h** and **3e** equal to 0.1 × IC_{50} and 1 × IC_{50}. The final concentration of MAO-A and –B were 0.0075 mg/mL and the concentrations of kynuramine were 45 µM and 30 µM for MAO-A and –B, respectively. The reactions were incubated for a further 20 min at 37 °C, terminated and the residual rates of 4-hydroxyquinoline formation were measured as described above. The residual enzyme catalytic rates were expressed as mean ± SD.

4.4.5. QSAR study

The values of the substituent descriptors σ_p, F, π, E_s and V_w were obtained from standard compilations [29,30]. The Statistica software package (StatSoft Inc.) was used to perform the multiple linear regression analysis. To estimate the significance of the regression equations, the F statistic was employed. An F value higher than the critical F value (F_{max}) was judged to be significant. The F_{max} value for 95% significance for models constructed from eight log IC_{50} values (Tables 2 and 3) and which contains one descriptor (out of a possible five: σ_p, F, π, E_s, V_w) was calculated to be 20.62, while the F_{max} value for models containing two descriptors was calculated to be 20.85 [33].

4.4.6. Molecular modeling studies

The modeling studies were carried out in the Windows based Discovery Studio 3.1 modeling software (Accelrys) [34]. The structure of the ligand, compound **3e**, was constructed within Discovery Studio and hydrogen atoms were added to the structure according to the appropriate protonation states at pH 7.4. The geometry of the ligand was briefly optimized in Discovery Studio using a Dreiding-like forcefield (5000

iterations) and atom potential types and partial charges were assigned with the Momany and Rone CHARMm forcefield. The crystallographic models of MAO-A (PDB code, 2Z5X) [36] and MAO-B (PDB code, 2V60) [37] were obtained from the Brookhaven Protein Data Bank. The pKa values and protonation states of the ionizable amino acids were calculated and hydrogen atoms were added at pH 7.4 to the models. The valences of the FAD cofactors (oxidized state) and cocrystallized ligands were corrected and the enzyme models were automatically typed with the Momany and Rone CHARMm forcefield. A fixed atom constraint was applied to the backbone of the enzymes and the models were energy minimized using the Smart Minimizer algorithm with the maximum steps set to 50000. For this procedure the implicit generalized Born solvation model with molecular volume was used. The cocrystallized inhibitors, waters and the backbone constraints were subsequently deleted from the models and the binding sites were identified from the enzyme cavities. The following active site waters are considered conserved and were retained for the docking calculations: In the MAO-B active site, HOH 1159, 1166 and 1309 in the A-chain of 2V60 [37]; In the MAO-A active site, HOH 710, 718 and 739 of 2Z5X. Docking was subsequently carried out with the CDOCKER algorithm with the generation of 10 random ligand conformations and a heating target temperature of 700 K in full potential mode. The docking solutions were finally refined using in situ ligand minimization employing the Smart Minimizer algorithm. Unless otherwise specified, all the application modules within Discovery Studio were set to their default values. The illustrations were generated with PyMOL [44].

Acknowledgements

The NMR spectra were recorded by André Joubert of the SASOL Centre for Chemistry, North-West University while the MS spectra were recorded by Marelize Ferreira of the Mass Spectrometry Service, University of the Witwatersrand. This work was supported by grants from the National Research Foundation and the Medical Research Council, South Africa. The financial assistance of the National Research Foundation (DAAD-NRF) towards this research is hereby acknowledged. Opinions expressed and conclusions arrived at, are those of the authors and are not necessarily to be attributed to the DAAD-NRF.

References

[1] M.B.H. Youdim, Y.S. Bakhle, Monoamine oxidase: Isoforms and inhibitors in Parkinson's disease and depressive illness, Br. J. Pharmacol. 147 (2006) S287.

[2] J.C. Shih, K. Chen, M.J Ridd, Monoamine oxidase: from genes to behavior, Annu. Rev. Neurosci. 22 (1999) 197-217.

[3] M.B.H. Youdim, D.E. Edmondson, K.F. Tipton, The therapeutic potential of monoamine oxidase inhibitors, Nat. Rev. Neurosci. 7 (2006) 295-309.

[4] M.B.H. Youdim, M. Weinstock, Therapeutic applications of selective and non-selective inhibitors of monoamine oxidase A and B that do not cause significant tyramine potentiation, Neurotox. 25 (2004) 243-250.

[5] P. Riederer, W. Danielczyk, E. Grünblatt, Monoamine oxdase-B inhibition in Alzheimer’s disase, Neurotox. 25 (2004) 271-277.

[6] U. Bonnet, Moclobemide: therapeutic use and clinical studies, CNS. Drug. Rev. 9 (2003) 97-140.

[7] H.H. Fernandez, J.J. Chen, Monoamine oxidase-B inhibition in the treatment of Parkinson's disease, Pharmacotherapy. 27 (2007) 174S.

[8] *P. Riederer, M.B.H. Youdim,* Monoamine oxidase activity and monoamine metabolism in brains of parkinsonian patients treated with l-deprenyl, J. Neurochem. 46 (1986) 1359-1365.

[9] J.P. Finberg, J. Wang, K. Bankiewich, J. Harvey-White, I.J. Kopin, D.S. Goldstein, Increased striatal dopamine production from L-DOPA following selective inhibition of monoamine oxidase B by R(+)-*N*-propargyl-1-aminoindan (rasagiline) in the monkey*, J. Neural Transm. Suppl. 52 (1998) 279.*

[10] D.A. Di Monte, L.E. DeLanney, I. Irwin, J.E. Royland, P. Chan, M.W. Jacowec, J.W. Langston, Monoamine oxidase-dependent metabolism of dopamine in the striatum and substantia nigra of L-DOPA-treated monkeys, Brain Res. 738 (1996) 53-59.

[11] M. Gesi, A. Santinami, R. Ruffoli, G. Conti, F. Fornai, Novel Aspects of Dopamine Oxidative Metabolism (Confounding Outcomes Take Place of Certainties, Pharmacol. Toxicol. 89 (2001) 217-224.

[12] F. Fornai, G. Battaglia, M. Gesi, F.S. Giorgi, F. Orzi, F. Nicoletti, Time-course and dose-response study on the effects of chronic L-DOPA administration on striatal dopamine levels and dopamine transporter following MPTP toxicity, Brain Res. 887 (2000) 110-117.

[13] S.A. Marchitti, R.A. Deitrich, V. Vasiliou, Neurotoxicity and metabolism of the catecholamine-derived 3,4-dihydroxyphenylacetaldehyde and 3,4-dihydroxyphenylglycolaldehyde: The role of aldehyde dehydrogenase, Pharmacol. Rev. 59 (2007) 125-150.

[14] J.M. Rabey, I. Sagi, M. Huberman, E. Melamed, A. Korczyn, N. Giladi, R. Inzelberg, R. Djaldetti, C. Klein, G. Berecz, Rasagiline mesylate, a new MAO-B inhibitor for the treatment of parkinson's disease: A double-blind study as adjunctive therapy to levodopa, Clin. Neuropharmacol. 23 (2000) 324-330.

[15] K.F. Tipton, S. Boyce, J. O'Sullivan, G.P. Davey, J. Healy, Monoamine oxidases: Certainties and uncertainties, Curr. Med. Chem. 11 (2004) 1965-1982.

[16] J.S. Fowler, N.D. Volkow, J. Logan, G. Wang, R.R. MacGregor, D. Schlyer, A.P. Wolf, N. Pappas, D. Alexoff, C. Shea, E. Dorflinger, L. Kruchowy, K. Yoo, E. Fazzini, C. Patlak, Slow recovery of human brain MAO B after L-deprenyl (selegeline) withdrawal, Synaps. 18 (1994) 86-93.

[17] B. Strydom, S.F. Malan, N. Castagnoli, J.J. Bergh, J.P. Petzer, Inhibition of monoamine oxidase by 8-benzyloxycaffeine analogues, Bioorg. Med. Chem. 18 (2010) 1018-1028.

[18] B. Strydom, J.J Bergh, J.P. Petzer, 8-Aryl- and alkyloxycaffeine analogues as inhibitors of monoamine oxidase, Eur. J. Med. Chem. 46 (2011) 3474-3485.

[19] H.P. Booysen, C. Moraal, G. Terre'blanche, A. Petzer, J.J. Bergh, J.P. Petzer, Thio- and aminocaffeine analogues as inhibitors of human monoamine oxidase, Bioorg. Med. Chem. 19 (2011) 7507-7518.

[20] J. Pretorius, S.F. Malan, N. Castagnoli, J.J. Bergh, J.P. Petzer, Dual inhibition of monoamine oxidase B and antagonism of the adenosine A_{2A} receptor by (E,E)-8-(4-phenylbutadien-1-yl)caffeine analogues, Bioorg. Med. Chem. 16 (2008) 8676-8684.

[21] E.M. Van der Walt, E.M. Milczek, S.F. Malan, D.E. Edmondson, N. Castagnoli, J.J. Bergh, J.P. Petzer, Inhibition of monoamine oxidase by (E)-styrylisatin analogues, Bioorg. Med. Chem. Lett. 19 (2009) 2509-2513.

[22] N. Vlok, S.F. Malan, N. Castagnoli, J.J. Bergh, J.P. Petzer, Inhibition of monoamine oxidase B by analogues of the adenosine A2A receptor antagonist (E)-8-(3-chlorostyryl)caffeine (CSC), Bioorg. Med. Chem. 14 (2006) 3512-3521.

[23] J.F. Chen, S. Steyn, R. Staal, J.P. Petzer, K. Xu, C.J. Van der Schyf, K. Castagnoli, P.K. Sonsalla, N. Castagnoli, M.A. Schwarzschild, 8-(3-Chlorostyryl)caffeine may attenuate MPTP neurotoxicity through dual actions of monoamine oxidase inhibition and A_{2A} receptor antagonism, J. Biol. Chem. 277 (2002) 36040-36044.

[24] W. Baumann, Die nervenkrankenfürsorge der stadt essen, Z. Gesamte Neurol. Psychiatr. 15 (1913) 114-121.

[25] E. Fischer, L. Reese, Ueber Caffeïn, Xanthin und Guanin, Justus Liebigs Ann. Chem. 221 (1883) 336-344.

[26] A. Tsotinis, T. Calogeropoulou, M. Koufaki, C. Souli, J. Balzarini, E. De Clercq, A. Makriyannis, Synthesis and antiretroviral evaluation of new alkoxy and aryloxy phosphate derivatives of 3'-azido-3'-deoxythymidine, J. Med. Chem. 39 (1996) 3418-3422.

[27] D. Stenkamp, S.G. Mueller, P. Lustenberger, T. Lehmann-Lintz, G.J. Roth, K. Rudolf, M. Schindler, L. Thomas, R.R.H. Lotz, U.S. Appl. No. 11/104915-Alkyne compounds with MCH antagonistic activity and medicaments comprising these compounds, filed Apr. 13, 2005.

[28] L. Novaroli, M. Reist, E. Favre, A. Carotti, M. Catto, P.A. Carrupt, Human recombinant monoamine oxidase B as reliable and efficient enzyme source for inhibitor screening, Bioorg. Med. Chem. 13 (2005) 6212-6217.

[29] C. Hansch, A. Leo, Exploring QSAR. Fundamentals and applications in chemistry and biology, American Chemical Society, Washington DC, 1995, 1-124.

[30] H. Van de Waterbeemb, B. Testa, in: Advances in Drug Research, B. Testa, Ed.; Academic Press: London, 1987, 85-225.

[31] R.K. Nandigama, D.E. Edmondson, Structure−activity relations in the oxidation of phenethylamine analogues by recombinant human liver monoamine oxidase A, Biochemistry 39 (2000) 15258-15265.

[32] M.C. Walker, D.E Edmondson, Structure-activity relationships in the oxidation of benzylamine analogues by bovine liver mitochondrial monoamine oxidase B, Biochemistry 33 (1994) 7088-7098.

[33] D.J. Livinstone, D.W. Salt, Judging the significance of multiple linear regression models, J. Med. Chem. 48 (2005) 661-663.

[34] Accelrys Discovery Studio 1.7, Accelrys Software Inc., San Diego, CA, USA. 2006, http://www.accelrys.com.

[35] L.J. legoaba, A. Petzer, J.P. Petzer, Inhibition of monoamine oxidase by selected C6-substituted chromone derivatives, Eur. J. Med. Chem. 49 (2012) 343-353.

[36] S.-Y. Son, J. Ma, Y. Kondou, M. Yoshimura, E. Yamashita, T. Tsukihara, Structure of human monoamine oxidase A at 2.2-A resolution: the control of opening the entry for substrates/inhibitors, Proc. Natl. Acad. Sci. U.S.A. 105 (2008) 5739-5744.

[37] C. Binda, J. Wang, L. Pisani, C. Caccia, A. Carotti, P. Salvati, D.E. Edmondson, A. Mattevi, Structures of human monoamine oxidase B complexes with selective noncovalent inhibitors: Safinamide and coumarin analogs, J. Med. Chem. 50 (2007) 5848-5852.

[38] C. Binda, P. Newton-Vinson, F. Hubalek, D.E. Edmondson, A. Mattevi, Structure of human monoamine oxidase B, a drug target for the treatment of neurological disorders, Nature Struct. Biol. 9 (2002) 22-26.

[39] L. Novaroli, A. Daina, E. Favre, J. Bravo, A. Carotti, F. Leonetti, M. Catto, P. Carrupt, M. Reist, Impact of species-dependent differences on screening, design, and development of MAO B inhibitors, J. Med. Chem. 49 (2005) 626-6272.

[40] F. Hubálek, C. Binda, A. Khalil, M. Li, A. Mattevi, N. Castagnoli, D.E. Edmondson, Demonstration of isoleucine 199 as a structural determinant for the selective inhibition of human monoamine oxidase B by specific reversible inhibitors, J. Biol. Chem. 280 (2005) 15761-15766.

[41] L. De Colibus, M. Li, C. Binda, A. Lustig, D.E. Edmondson, A. Mattevi, Three-dimensional structure of human monoamine oxidase A (MAO A): Relation to the structures of rat MAO A and human MAO B, PNAS, 102 (2005) 12684-12689.

[42] M. Sono, N. Toyoda, K. Shimizu, E. Noda, Y. Shizuri, M. Tori, Functionalization including fluorination of nitrogen-containing compounds using electrochemical oxidation, Chem. Pharm. Bull. 44 (1996) 1141-1145.

[43] R.C. Huston, W.F. Allen, Caffeine derivatives. I. The 8-ethers of caffeine, 56 (1934) 1356-1358.

[44] W.L. DeLano, The PyMOL Molecular Graphics System. DeLano Scientific, San Carlos, USA, 2002.

Supplementary Material

S1: HPLC traces

Method: To determine the purity of the previously unreported compounds, HPLC analyses were carried out. HPLC analyses were performed with an Agilent 1100 HPLC system equipped with a quaternary pump and an Agilent 1100 series diode array detector. A Venusil XBP C18 column (4.60 × 150 mm, 5 µm) was used and the mobile phase consisted initially of 30% acetonitrile and 70% MilliQ water at a flow rate of 1 mL/min. At the start of each HPLC run a solvent gradient program was initiated by linearly increasing the composition of the acetonitrile in the mobile phase to 85% acetonitrile over a period of 5 min. Each HPLC run lasted 15 min and a time period of 5 min was allowed for equilibration between runs. A volume of 20 µL of solutions of the test compounds in acetonitrile (200 µM) was injected into the HPLC system and the eluent was monitored at a wavelength of 254 nm.

8-[2-(4-Fluorophenoxy)ethoxy]caffeine (3d)

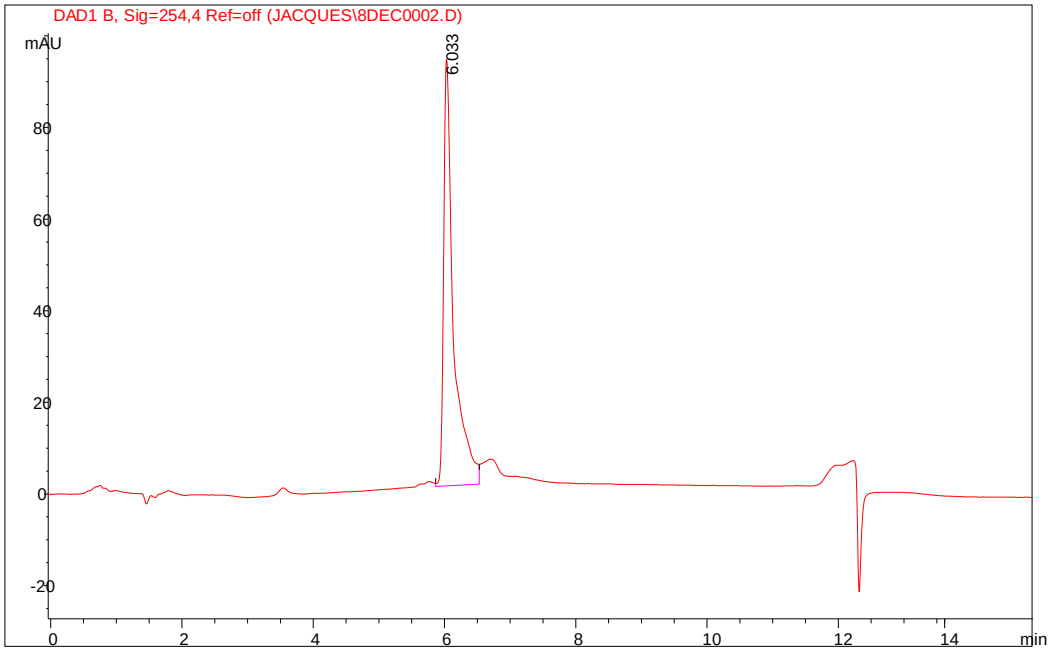

8-{2-[4-(Trifluoromethyl)phenoxy]ethoxy}caffeine (3e)

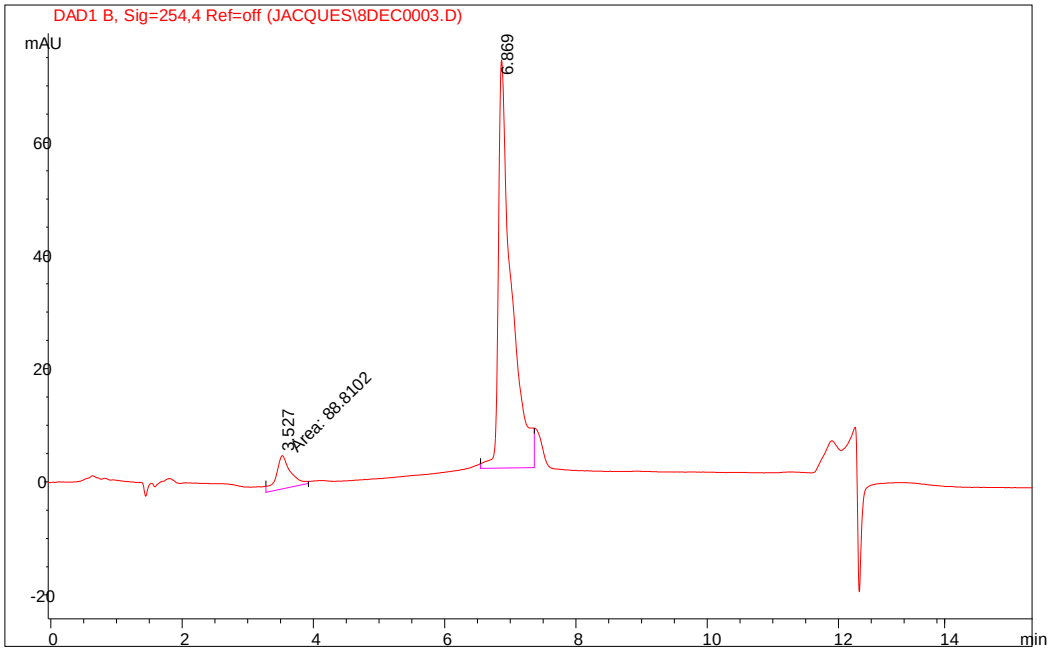

8-[2-(4-Methylphenoxy)ethoxy]caffeine (3f)

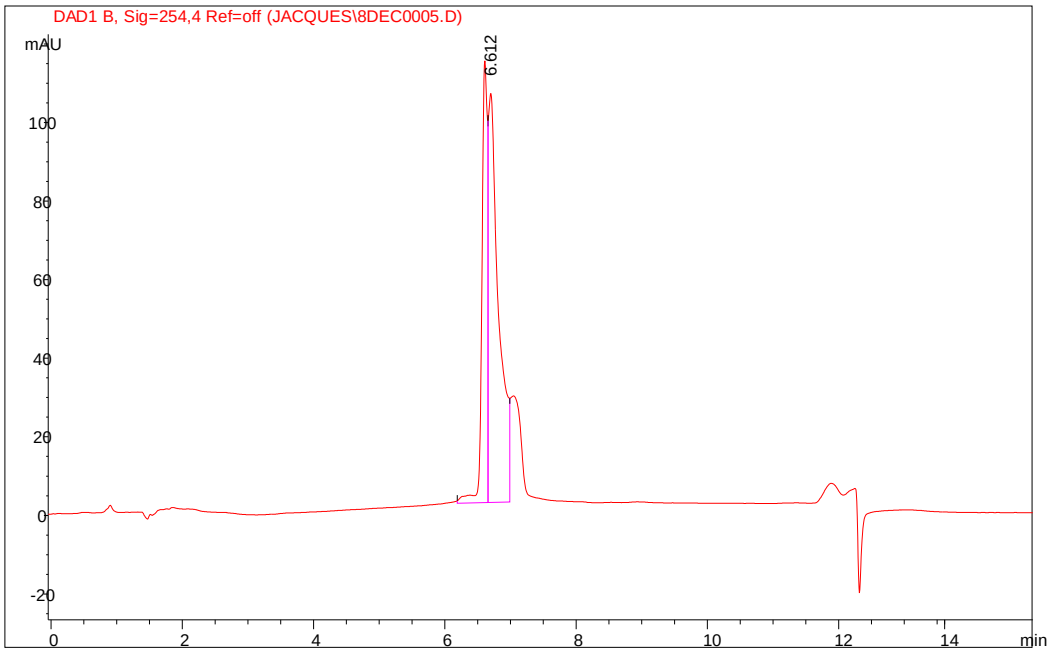

8-[2-(4-Methoxyphenoxy)ethoxy]caffeine (3g)

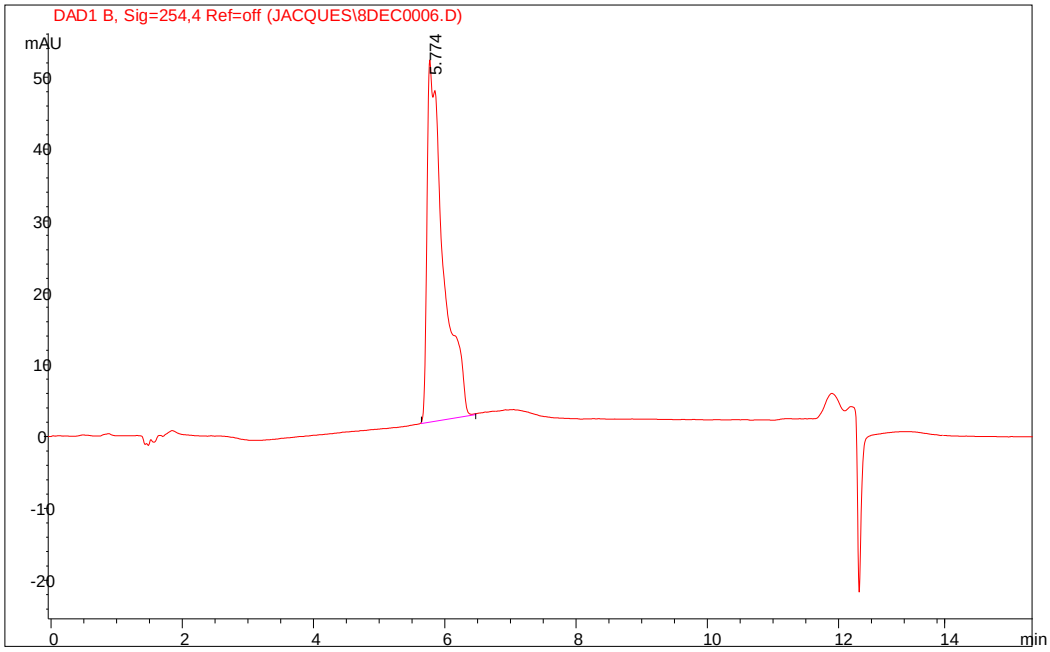

8-[2-(4-Iodophenoxy)ethoxy]caffeine (3h)

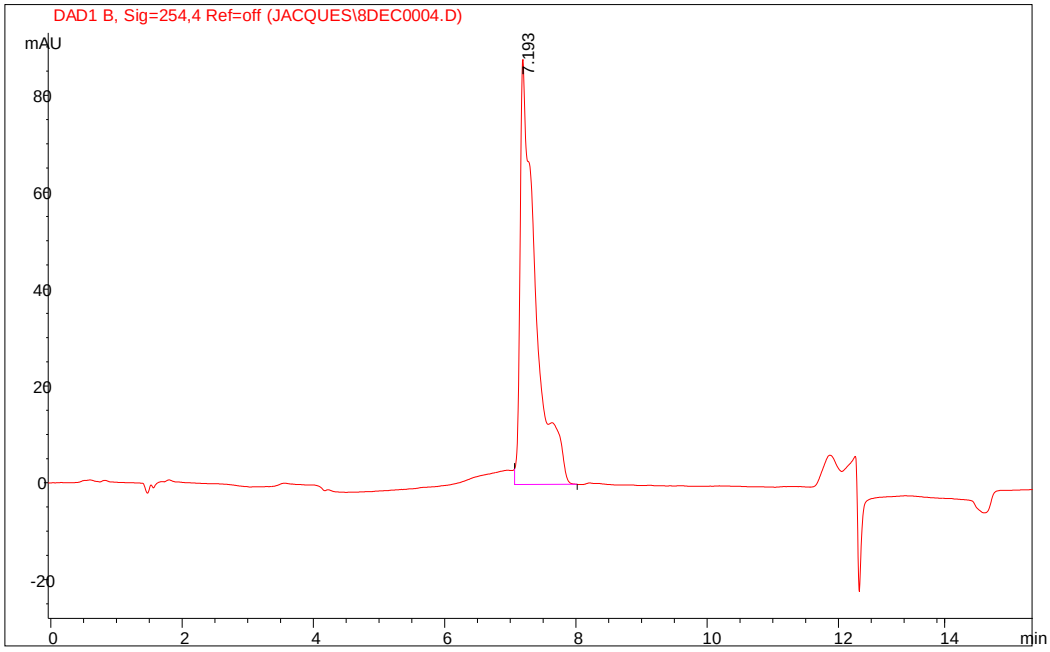

8-[2-(4-Cyanophenoxy)ethoxy]caffeine (3i)

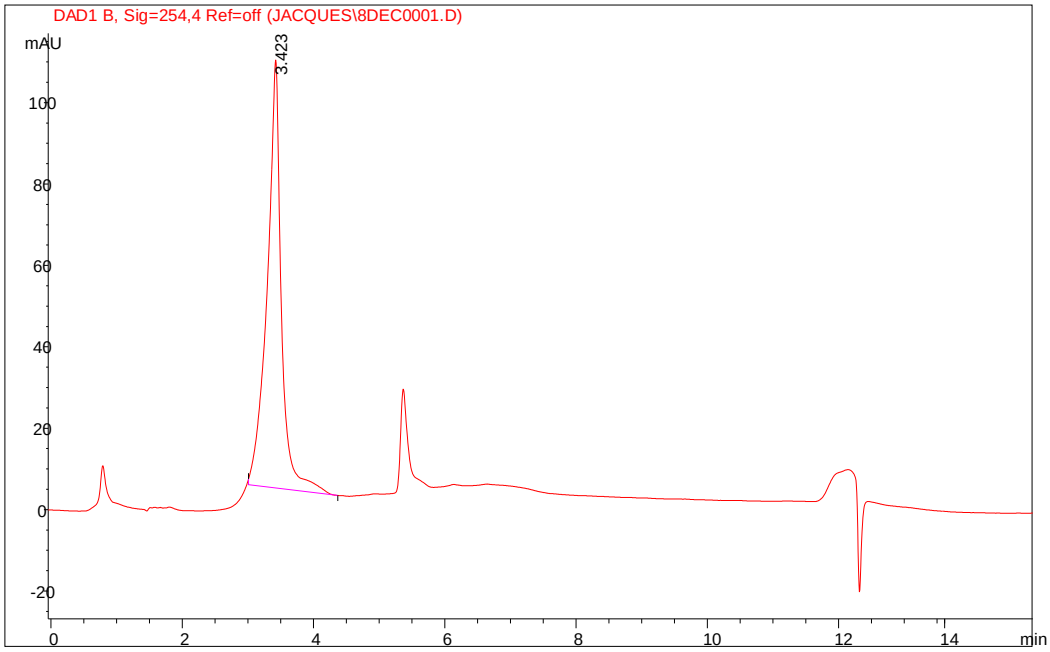

8-[2-(4-Nitrophenoxy)ethoxy]caffeine (3j)

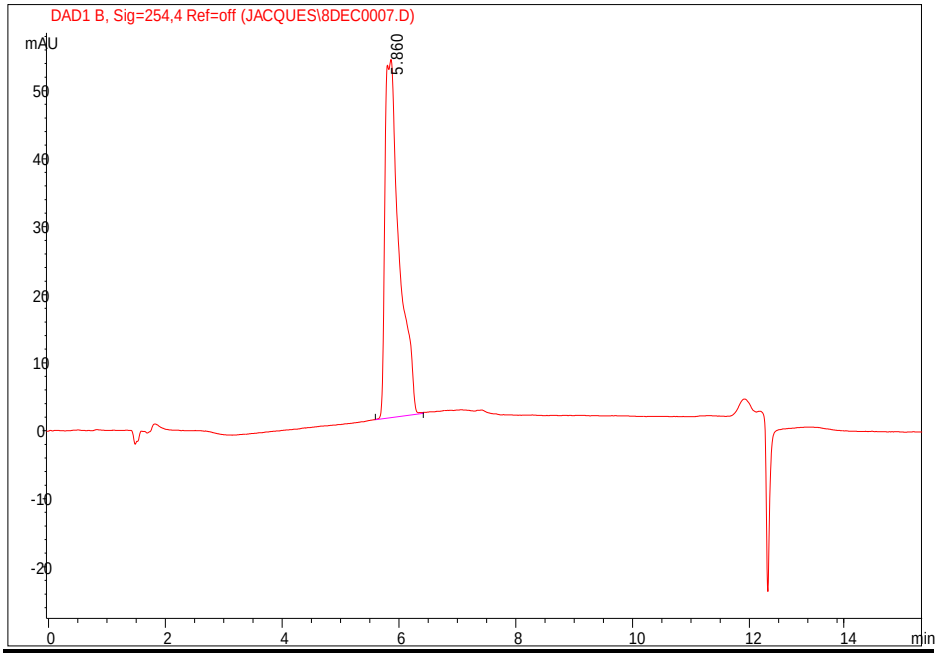

Acetonitrile

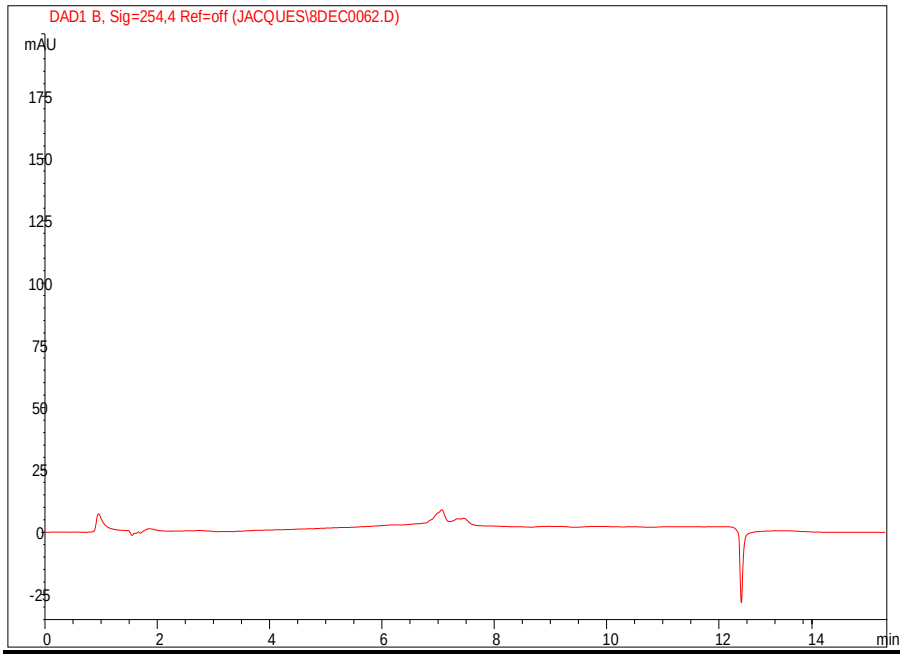

S2: ^{1}H NMR and ^{13}C NMR spectra

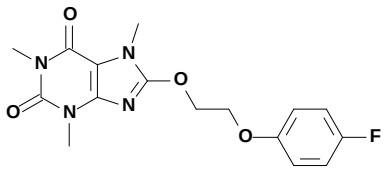

S2: ^{1}H NMR and ^{13}C NMR spectra

8-[2-(4-Fluorophenoxy)ethoxy]caffeine (**3d**)
^{1}H NMR

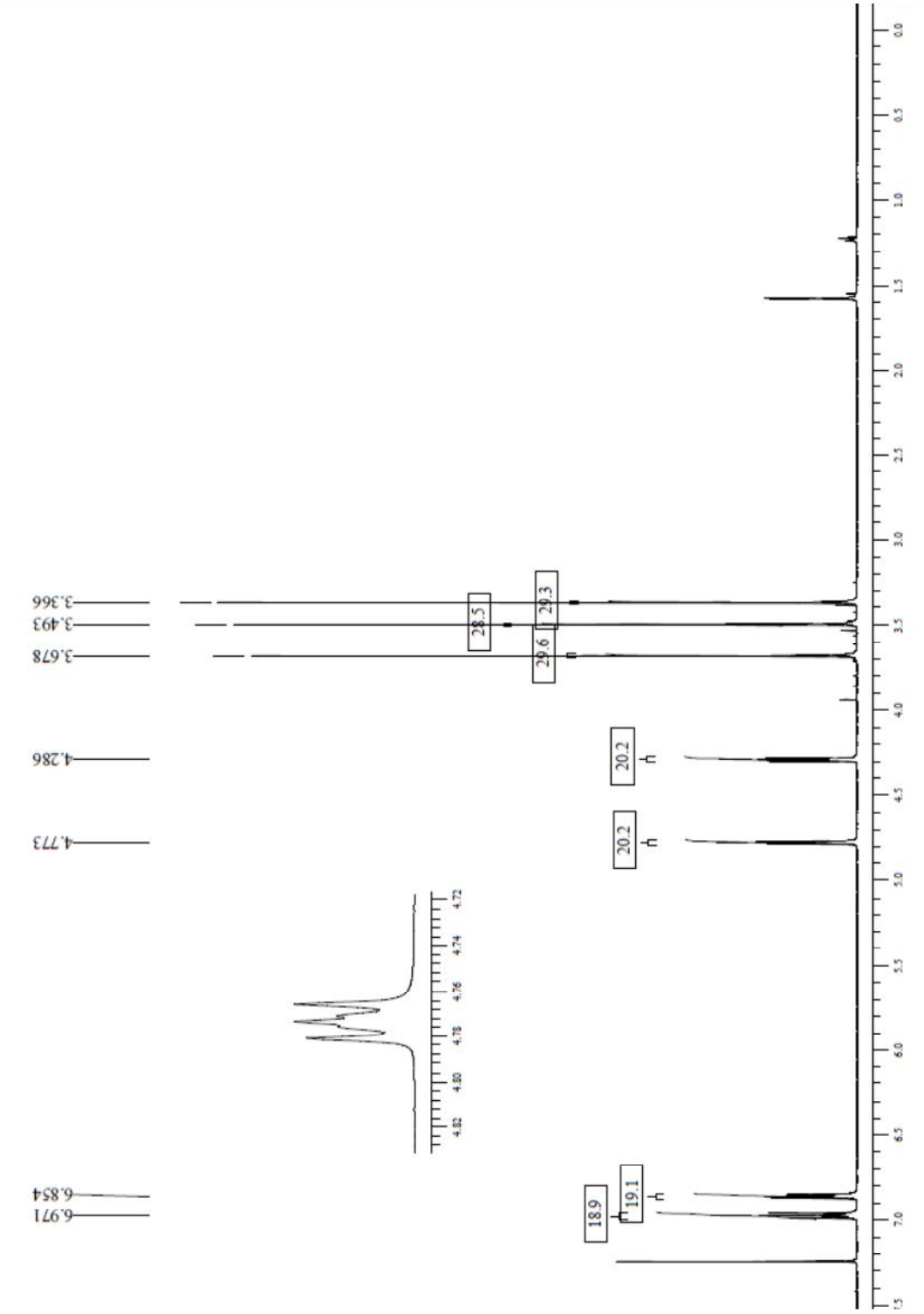

^{13}C NMR

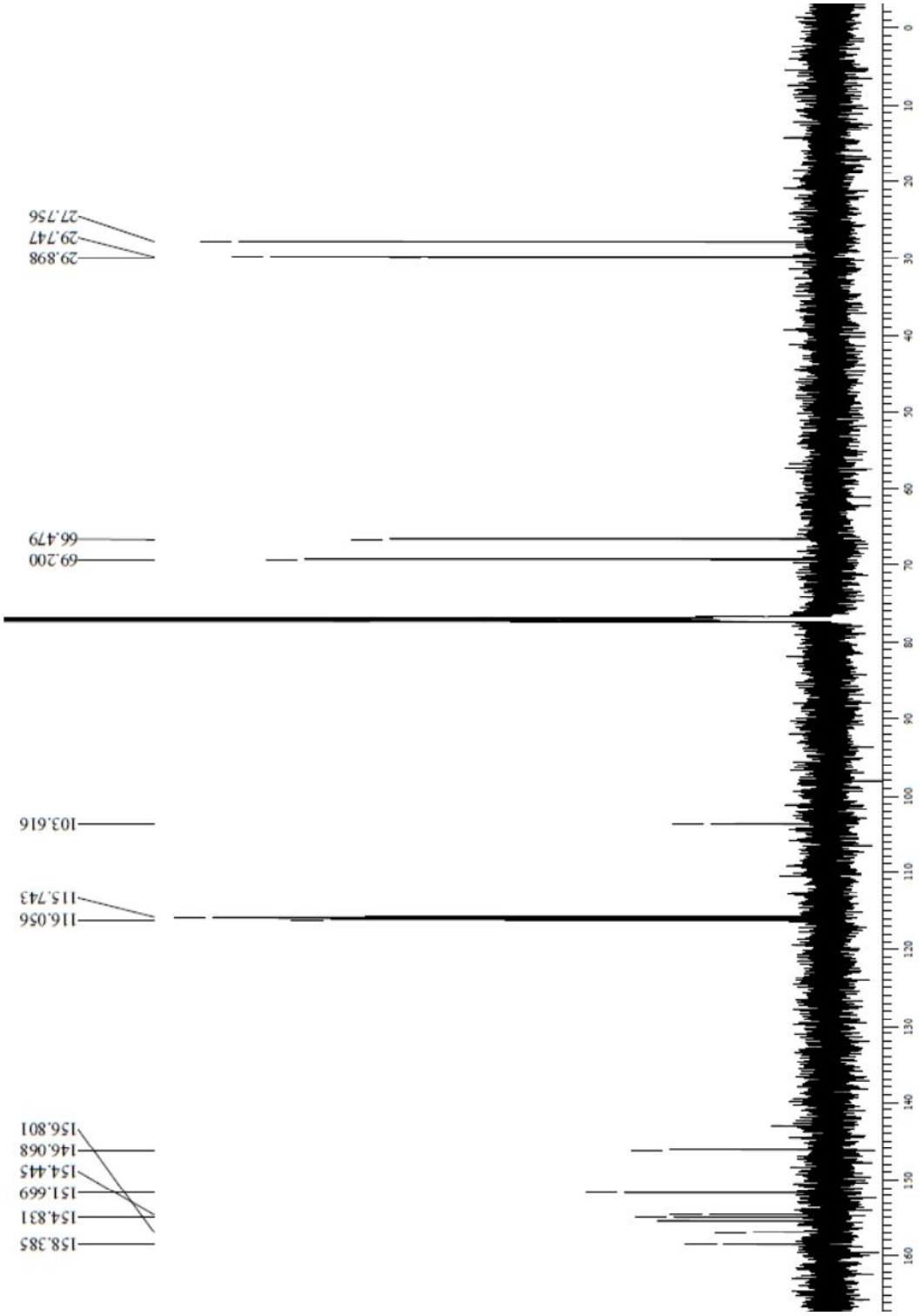
27.756
29.747
29.898
66.479
69.200
103.616
115.743
116.056
156.801
146.068
154.445
151.669
154.831
158.385

8-{2-[4-(Trifluoromethyl)phenoxy]ethoxy}caffeine (**3e**)
^{1}H NMR

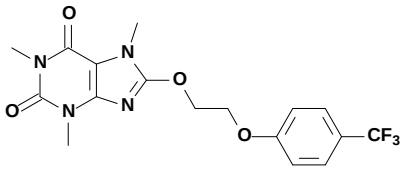

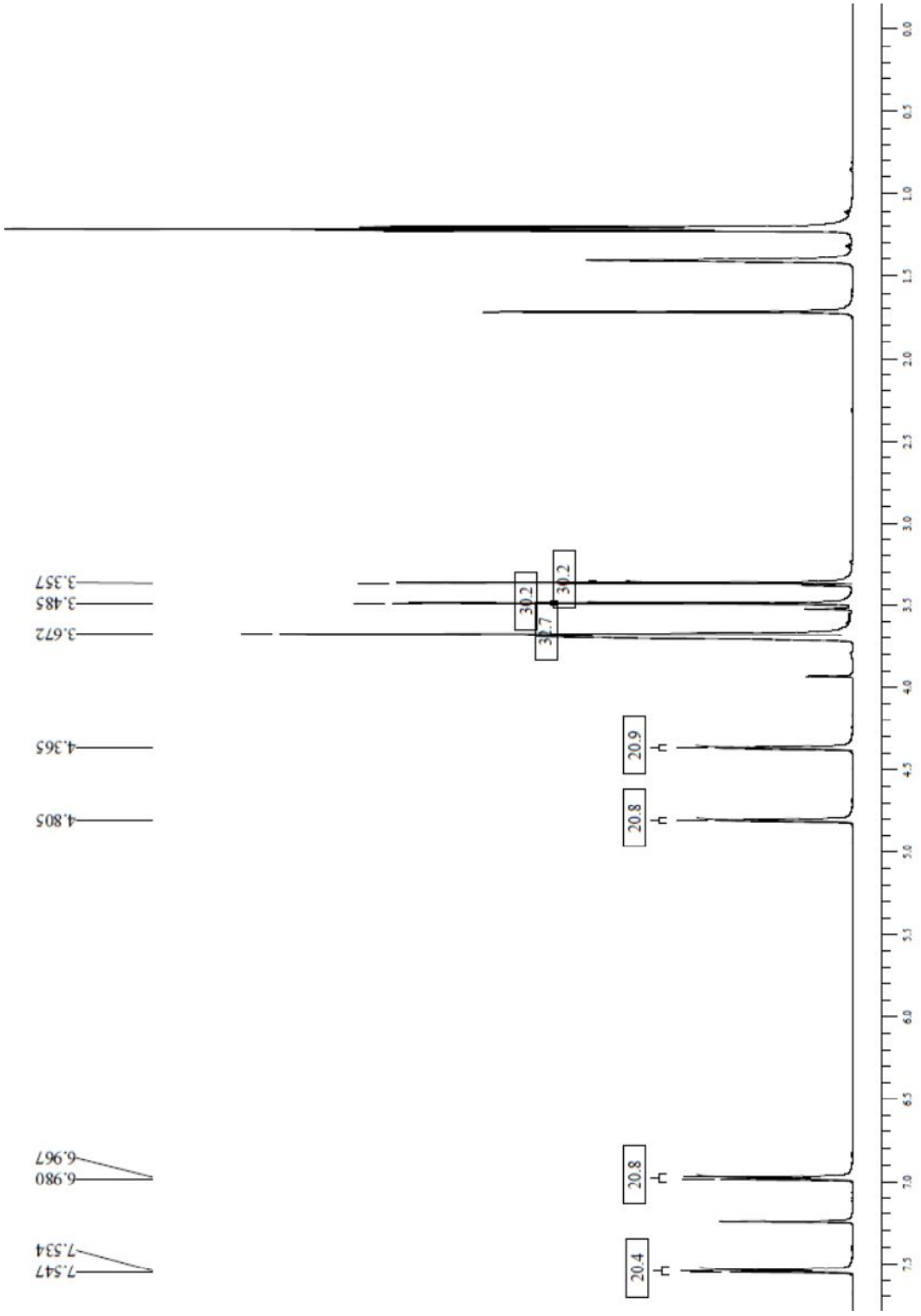

^{13}C NMR

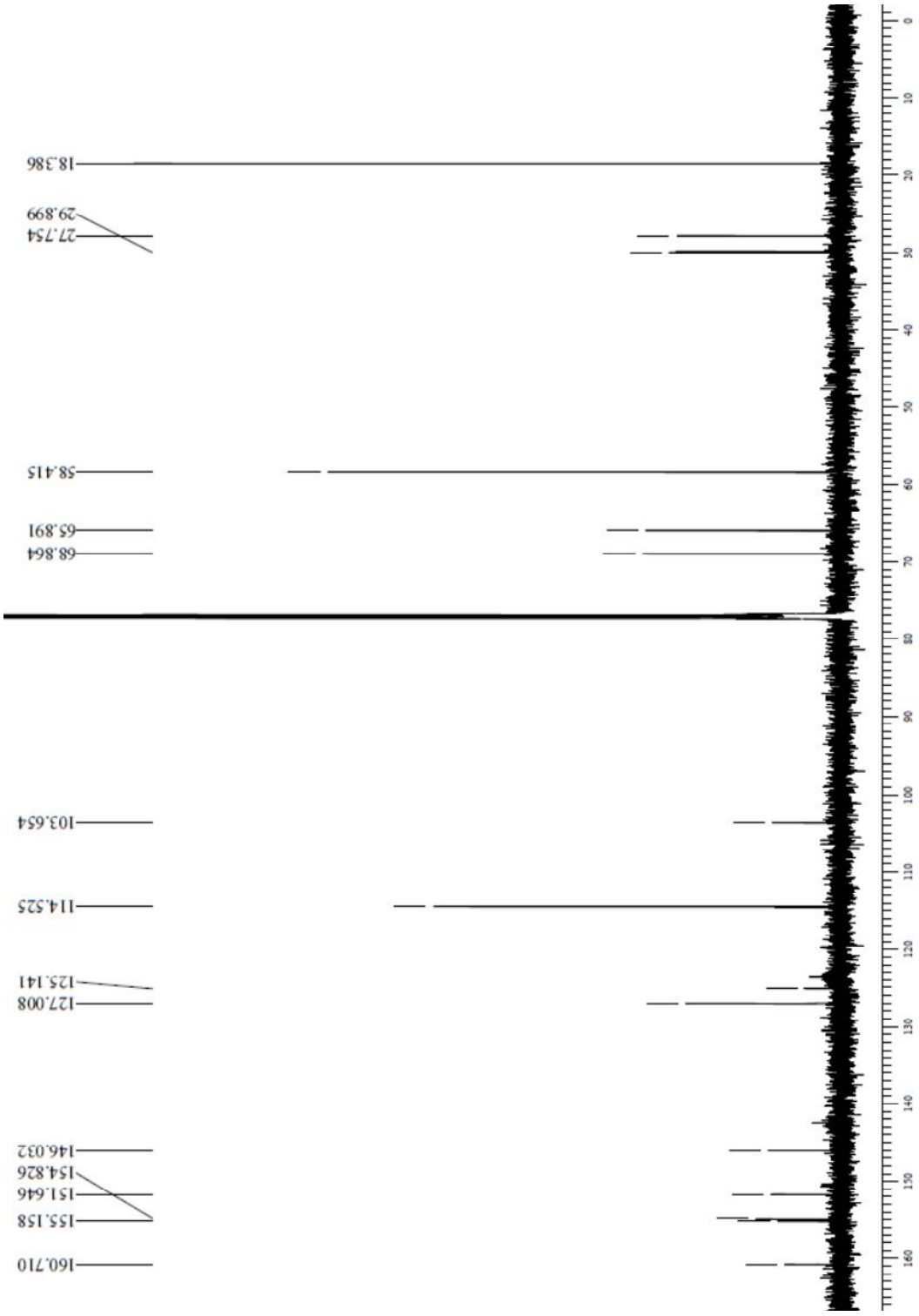
18.386
29.899
27.754
58.415
65.891
68.864
103.654
114.525
125.141
127.008
146.032
154.826
151.646
155.158
160.710

8-[2-(4-Methylphenoxy)ethoxy]caffeine (**5f**)
^{1}H NMR

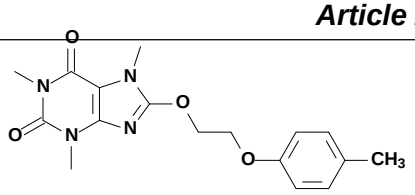

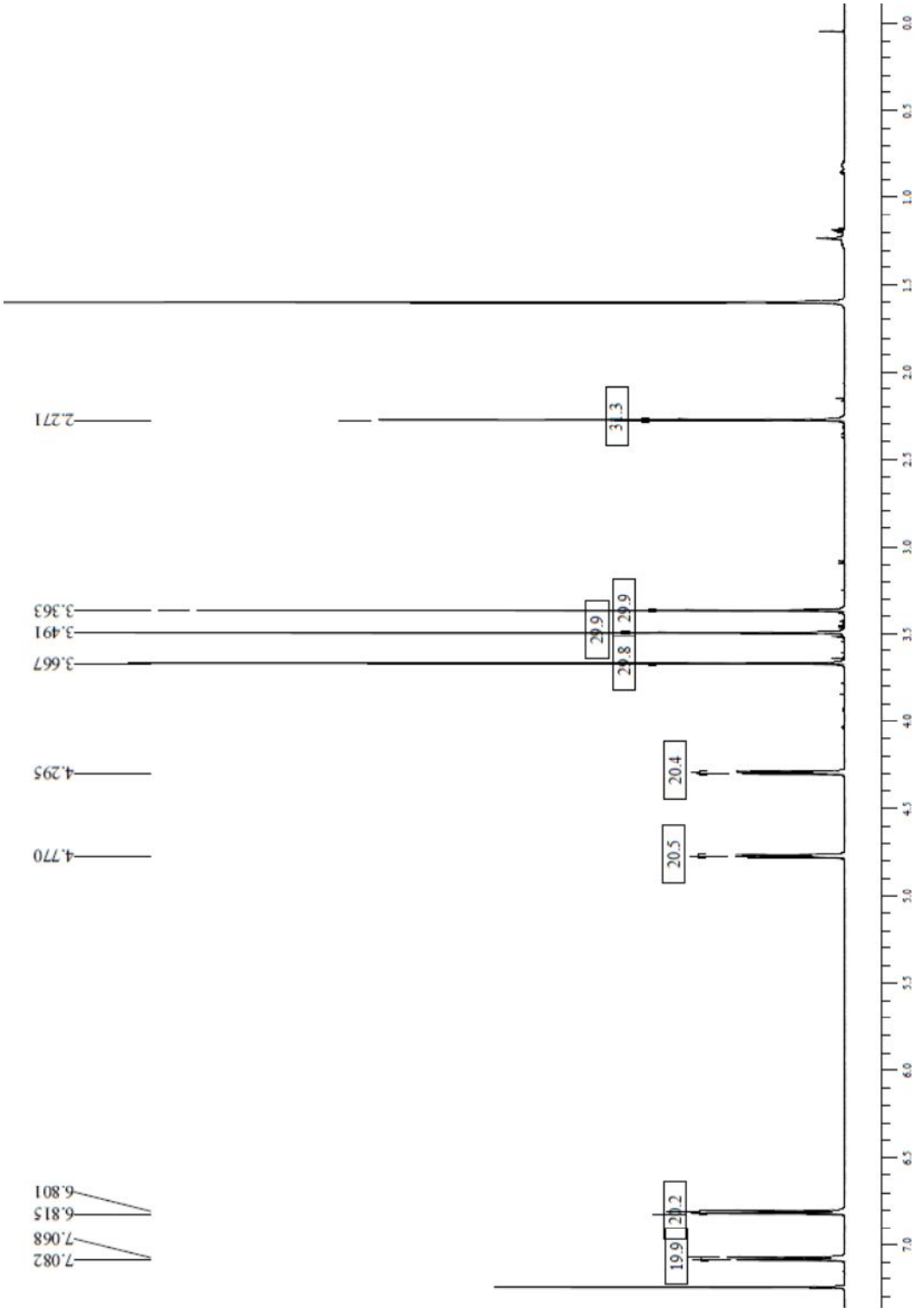

^{13}C NMR

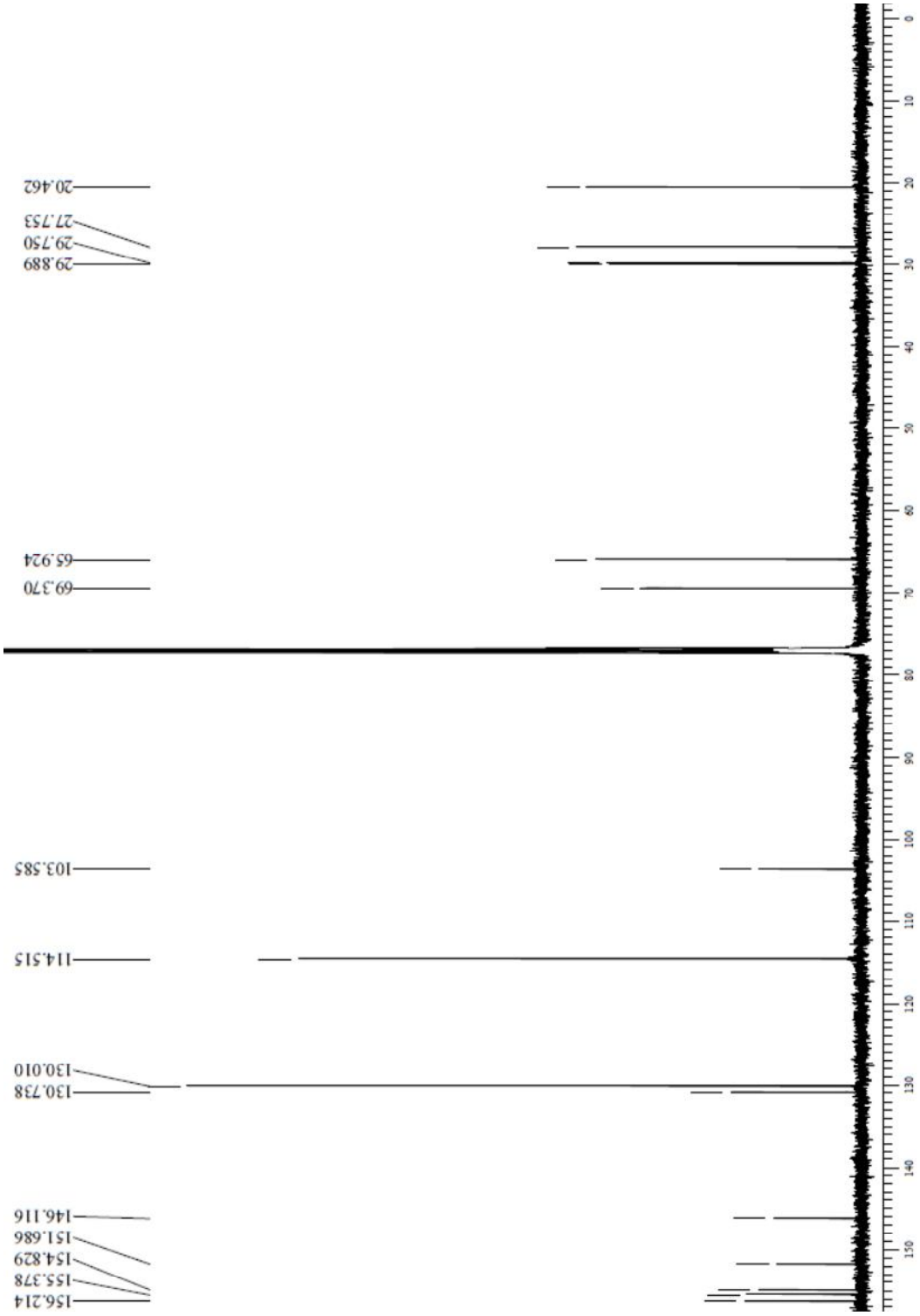
20.462
27.753
29.750
29.889
65.924
69.370
103.585
114.515
130.010
130.738
146.116
151.686
154.829
155.378
156.214

8-[2-(4-Methoxyphenoxy)ethoxy]caffeine (**5g**)
^{1}H NMR

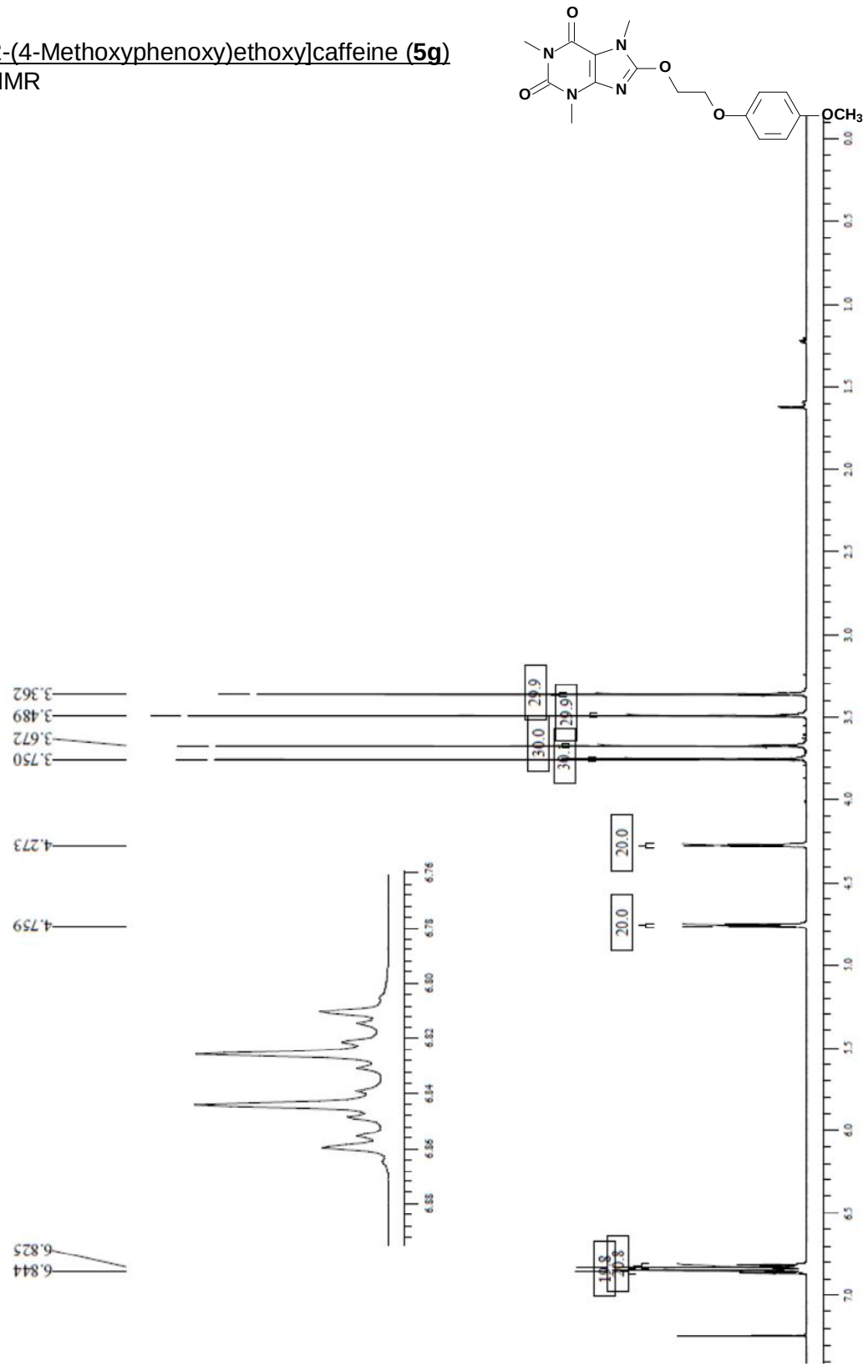

^{13}C NMR

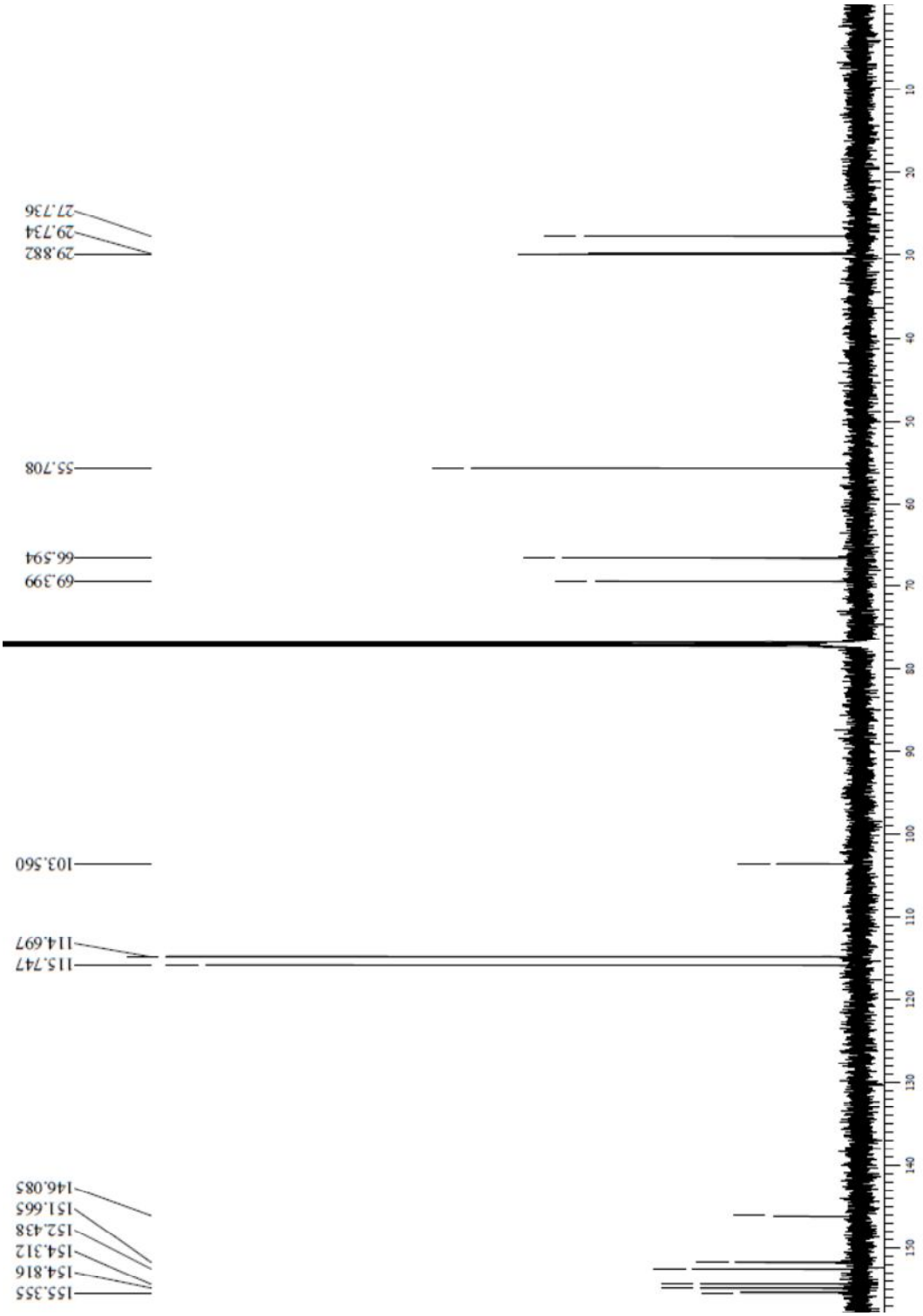
27.736
29.734
29.882
55.708
66.594
69.399
103.560
114.697
115.747
146.085
151.665
152.438
154.312
154.816
155.355

8-[2-(4-Iodophenoxy)ethoxy]caffeine (**5h**)
^{1}H NMR

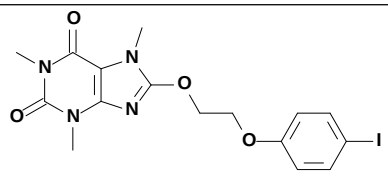

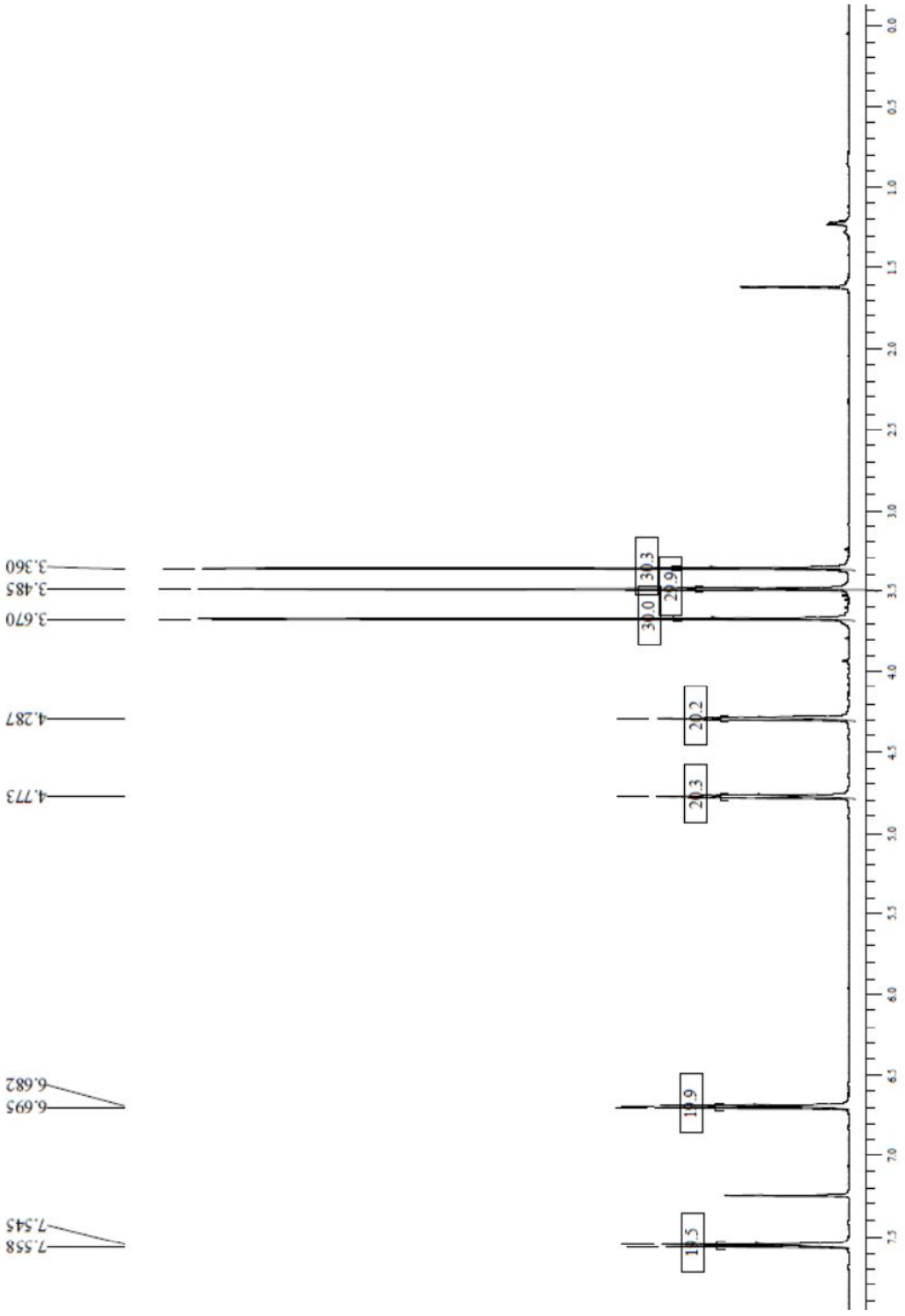

^{13}C NMR

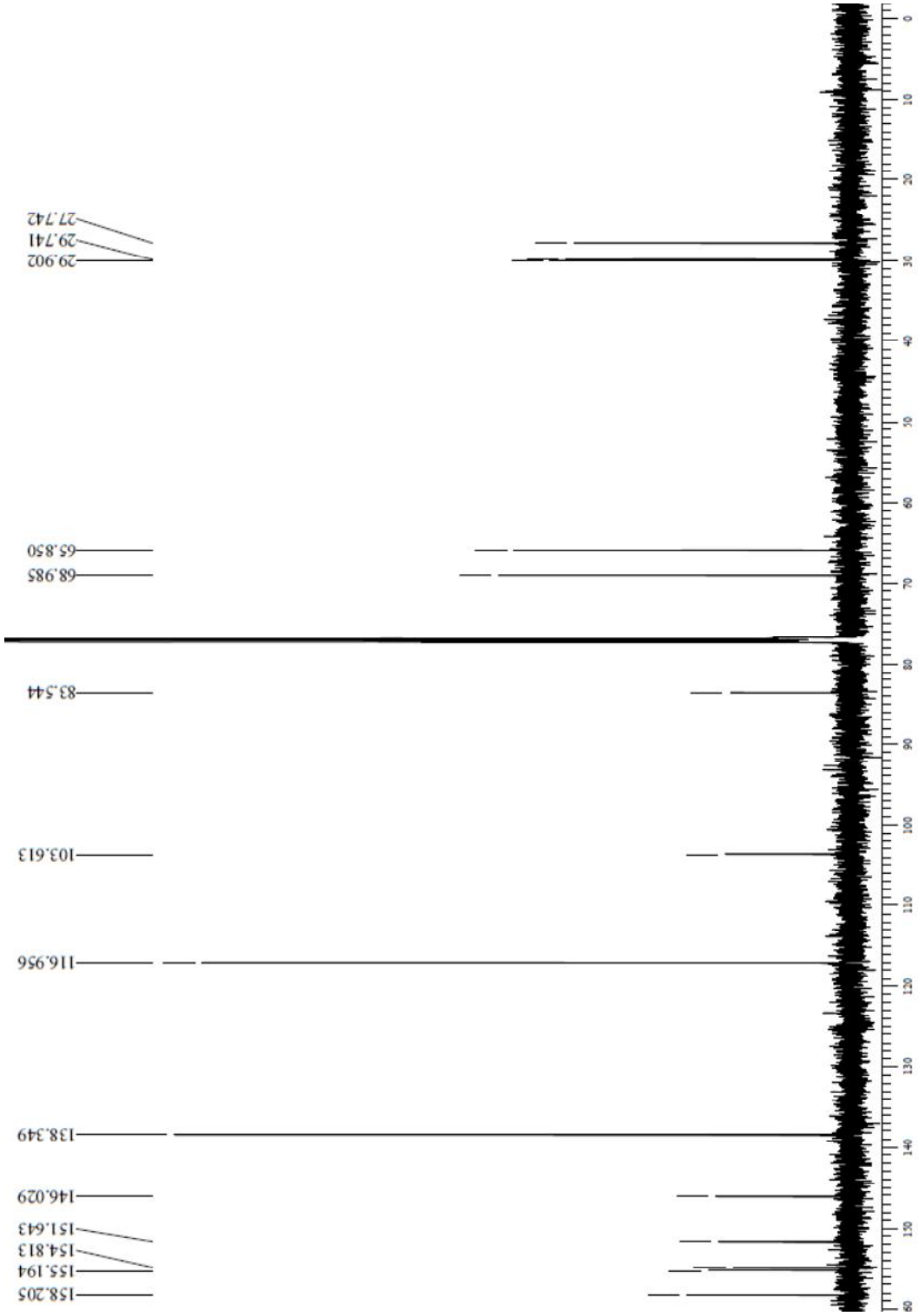
27.742
29.741
29.902
65.850
68.985
83.544
103.613
116.956
138.349
146.029
151.643
154.813
155.194
158.205

8-[2-(4-Cyanophenoxy)ethoxy]caffeine (**5i**)
^{1}H NMR

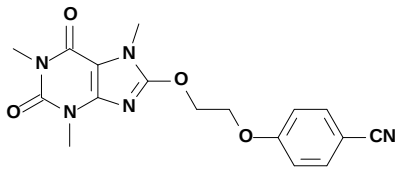

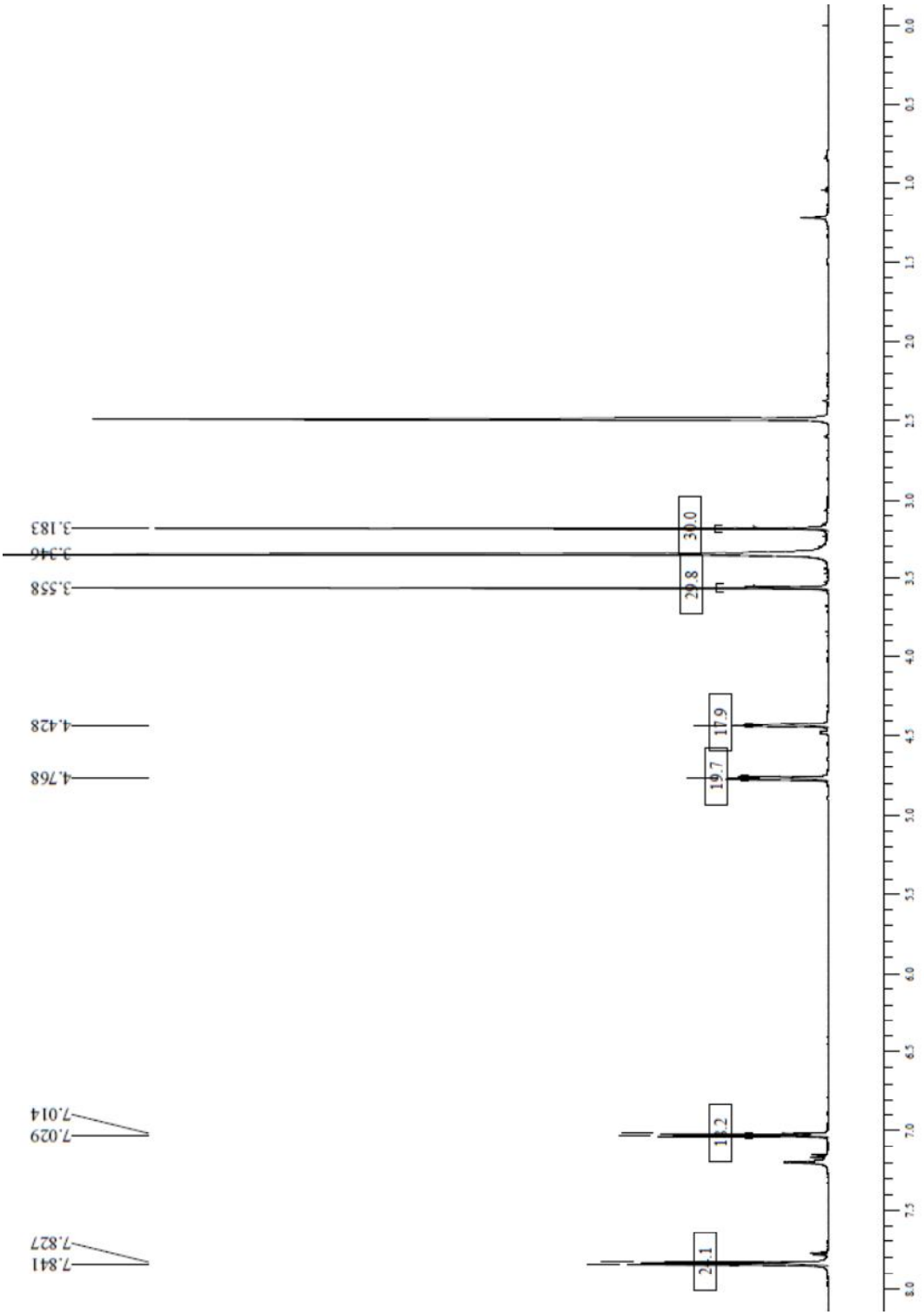

^{13}C NMR

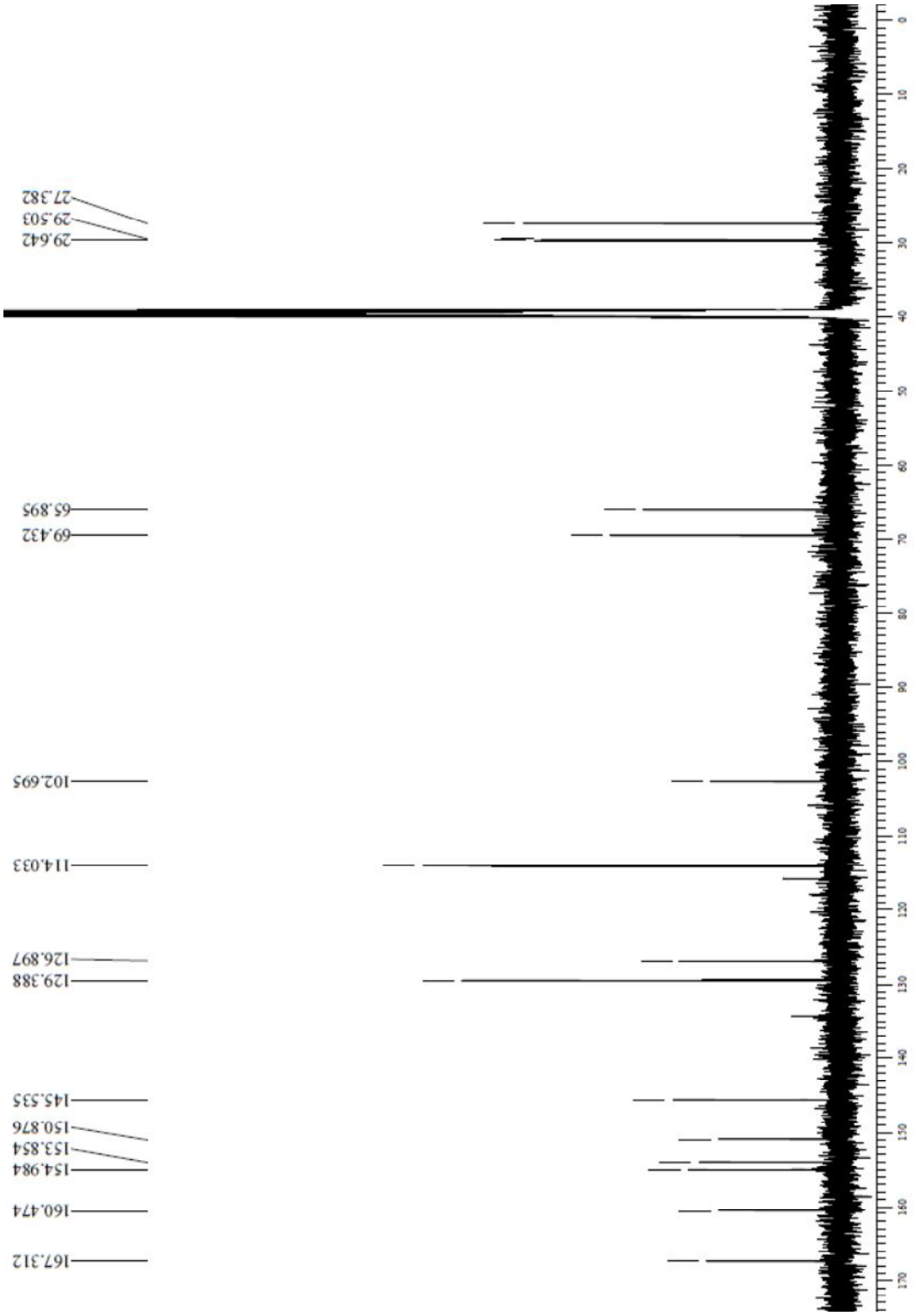
27.382
29.503
29.642
65.895
69.432
102.695
114.033
126.897
129.388
145.535
150.876
153.854
154.984
160.474
167.312

8-[2-(4-Nitrophenoxy)ethoxy]caffeine (**5j**)
^{1}H NMR

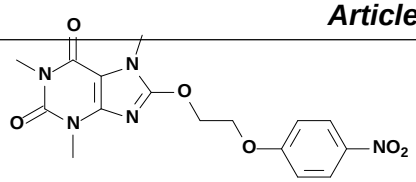

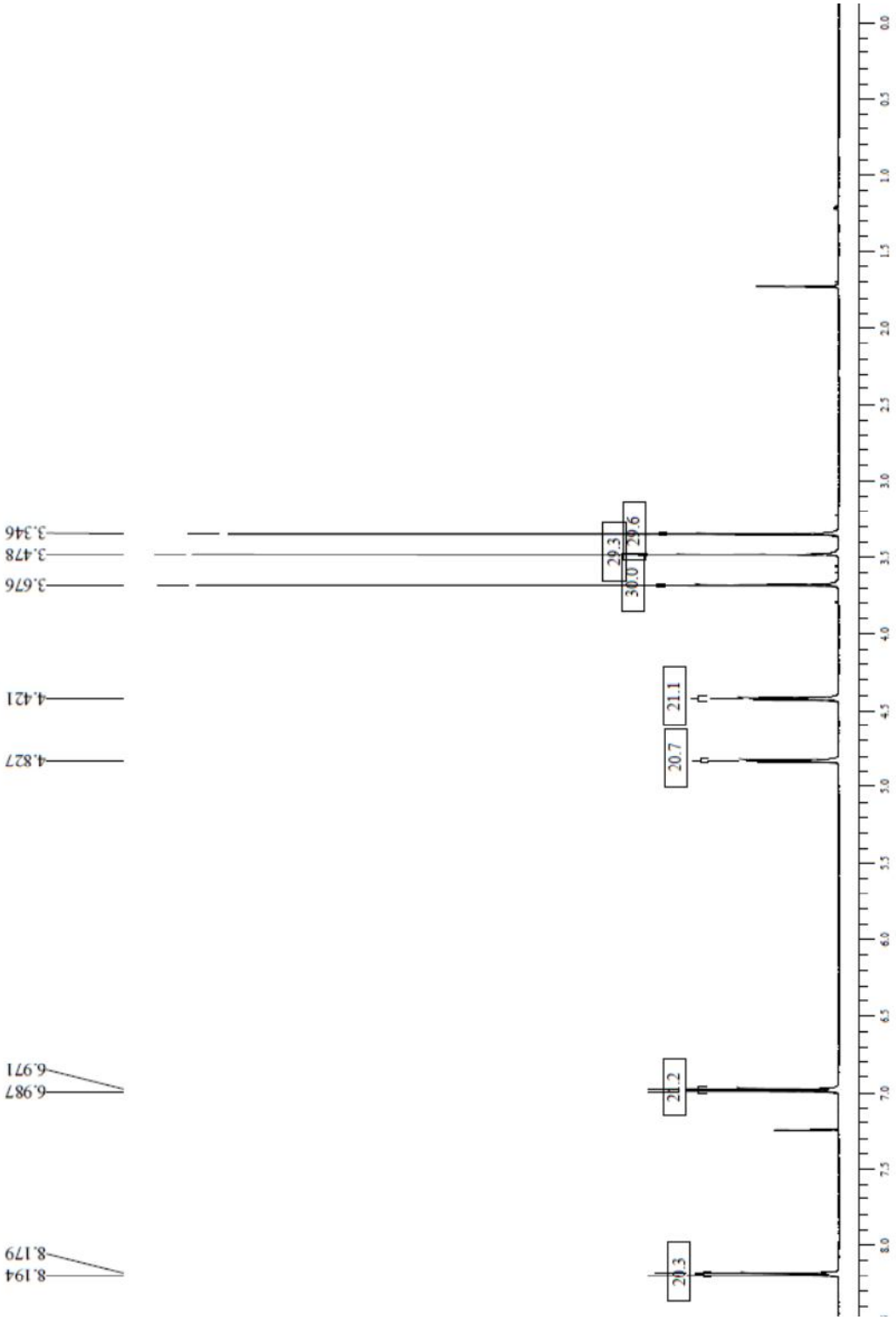

^{13}C NMR

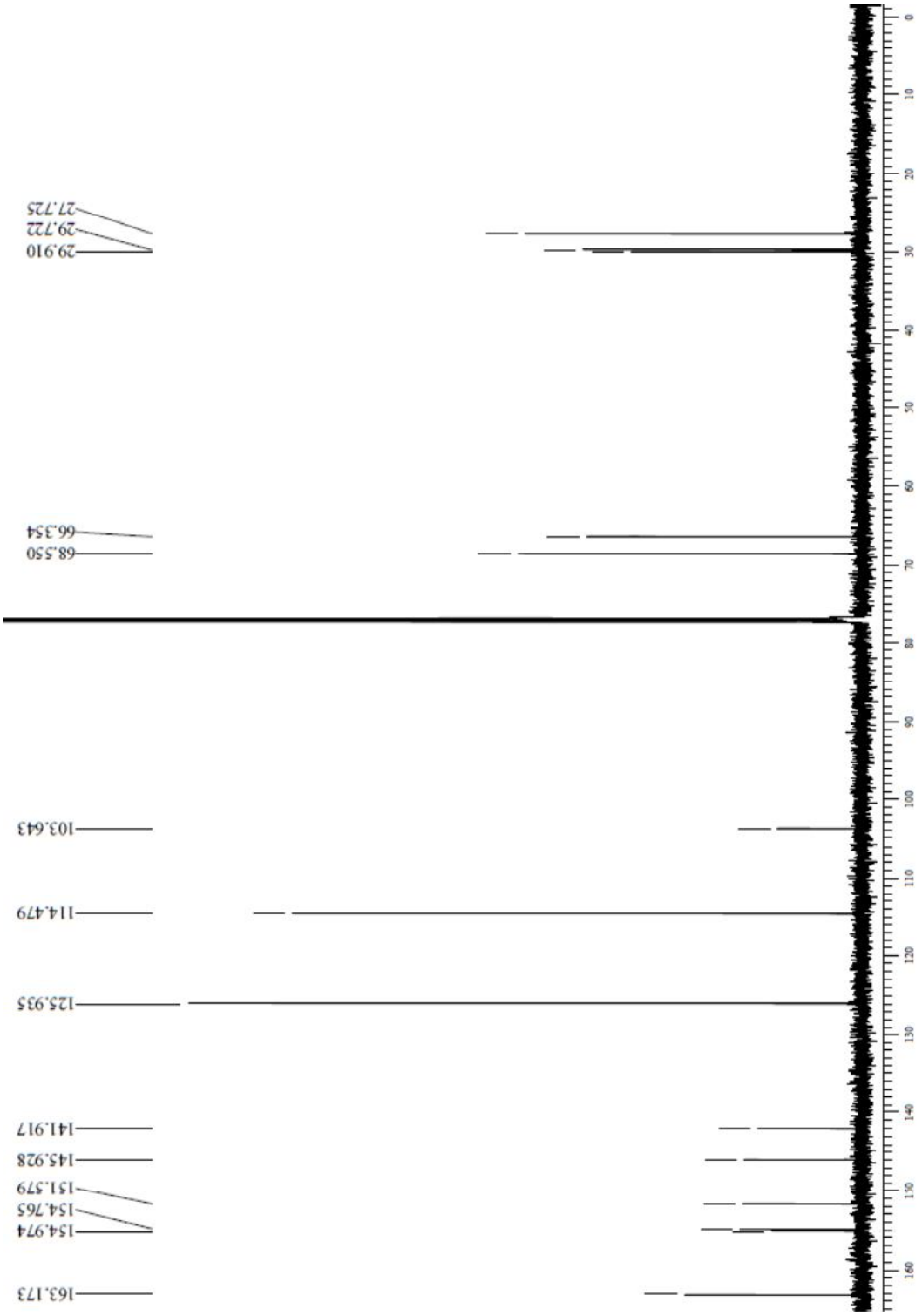
27.725
29.722
29.910
66.354
68.550
103.643
114.479
125.935
141.917
145.928
151.579
154.765
154.974
163.173